Land use/cover classification in the Brazilian Amazon using satellite images

Dengsheng Lu[1], Mateus Batistella[2], Guiying Li[1], Emilio Moran[1], Scott Hetrick[1], Corina da Costa Freitas[3], Luciano Vieira Dutra[3] and Sidnei João Siqueira Sant'Anna[3]

[1]Indiana University, Anthropological Center for Training and Research on Global Environmental Change, Student Building 331, 701 East Kirkwood Avenue, Bloomington, Indiana, 47405, USA. E-mail: dlu@indiana.edu, ligu@indiana.edu, moran@indiana.edu, shetrick@indiana.edu [2]Embrapa Monitoramento por Satélite, Avenida Soldado Passarinho, nº 303, CEP 13070-115 Campinas, SP, Brazil. E-mail: mb@cnpm.embrapa.br [3]Instituto Nacional de Pesquisas Espaciais, Avenida dos Astronautas, nº 1.758, CEP 12245-010 São José dos Campos, SP, Brazil. E-mail: corina@dpi.inpe.br, dutra@dpi.inpe.br, sidnei@dpi.inpe.br

Abstract – Land use/cover classification is one of the most important applications in remote sensing. However, mapping accurate land use/cover spatial distribution is a challenge, particularly in moist tropical regions, due to the complex biophysical environment and limitations of remote sensing data per se. This paper reviews experiments related to land use/cover classification in the Brazilian Amazon for a decade. Through comprehensive analysis of the classification results, it is concluded that spatial information inherent in remote sensing data plays an essential role in improving land use/cover classification. Incorporation of suitable textural images into multispectral bands and use of segmentation-based method are valuable ways to improve land use/cover classification, especially for high spatial resolution images. Data fusion of multi-resolution images within optical sensor data is vital for visual interpretation, but may not improve classification performance. In contrast, integration of optical and radar data did improve classification performance when the proper data fusion method was used. Among the classification algorithms available, the maximum likelihood classifier is still an important method for providing reasonably good accuracy, but nonparametric algorithms, such as classification tree analysis, have the potential to provide better results. However, they often require more time to achieve parametric optimization. Proper use of hierarchical-based methods is fundamental for developing accurate land use/cover classification, mainly from historical remotely sensed data.

Index terms: data fusion, multiple sensor data, nonparametric classifiers, texture.

Classificação de uso e cobertura da terra na Amazônia brasileira por meio de imagens de satélite

Resumo – A classificação de uso e cobertura da terra é uma das principais aplicações do sensoriamento remoto. Contudo, a precisão no mapeamento da distribuição espacial do uso/cobertura da terra é um desafio, principalmente em regiões tropicais úmidas, em razão do complexo ambiente biofísico e das limitações dos dados de sensoriamento remoto per se. Este trabalho revisa experimentos relacionados à classificação do uso/cobertura da terra na Amazônia brasileira, durante uma década. A partir de análise compreensiva dos resultados de classificação, conclui-se que a informação espacial, em dados de sensoriamento remoto, tem papel fundamental na melhoria da classificação de uso/cobertura da terra. A incorporação de imagens de textura, em bandas multiespectrais, e o uso de método baseado em segmentação são formas importantes de melhorar a classificação, especialmente para imagens de alta resolução espacial. A fusão de dados de imagens de resolução múltipla dentro de dados do sensor ótico é vital para a interpretação visual, mas pode não melhorar o desempenho da classificação. Em contraste, a integração de dados ópticos e de radar melhorou o desempenho da classificação, quando o método adequado de fusão de dados foi utilizado. Entre os algoritmos de classificação disponíveis, o classificador de máxima verossimilhança ainda é importante para se obter precisão razoável, mas algoritmos não paramétricos, como a análise por árvore de decisão, podem promover melhores resultados. Porém, algoritmos não paramétricos geralmente demandam mais tempo para obtenção da parametrização otimizada. O uso adequado de métodos baseados em hierarquia é fundamental para a precisão na classificação de uso/cobertura da terra, sobretudo em dados de sensoriamento remoto antigos.

Termos para indexação: fusão de dados, dados de sensor múltiplo, classificadores não paramétricos, textura.

Introduction

The Brazilian Amazon is the largest continuous primary forest in the world and has special importance for biodiversity, global nutrient cycles, and climate change. Since the 1970s deforestation has converted a large area of primary forest and cerrado (Brazilian savanna-like vegetation) into agriculture, pasture, secondary succession, and agroforestry (Cardille & Foley, 2003; Carreiras et al., 2006; Sano et al., 2010).

Therefore, monitoring of deforestation in the Brazilian Amazon has received great attention in the past two decades in programs such as Prodes, Program for the Estimation of Deforestation in the Brazilian Amazon (Brasil, 2012a), and DETER, Real Time Deforestation Monitoring System (Brasil, 2012b). Considering that the areas of secondary forest are vital as a carbon sink and the pressure from agricultural expansion, the mapping and monitoring of secondary forest and agricultural lands has grown in significance (Lu, 2005; Lobell & Asner, 2004; Galford et al., 2008; Wardlow & Egbert, 2008). However, the complex biophysical environment and the existence of highly diverse species make it challenging to obtain accurate land use/cover classifications with remotely sensed data.

Mapping of land use/cover distribution is one of the most important applications in remote sensing, and research on improving land use/cover classification has long been an active research topic. Significant progress has been achieved, including the development of: advanced classification algorithms, such as neural network, decision tree, support vector machine, object-based algorithms, sub-pixel based algorithms, and contextual algorithms (Tso & Mather, 2001; Franklin & Wulder, 2002; Frery et al., 2007; Lu & Weng, 2007; Rogan et al., 2008; Blaschke, 2010); techniques that incorporate multi-source data in a classification procedure, such as the integration of different spatial resolution or sensor images (Pohl & Van Genderen, 1998; Ehlers et al., 2010; Zhang, 2010) and the integration of remote sensing and ancillary data (Harris & Ventura, 1995; Li, 2010); and techniques for modifying classified images by using expert knowledge (Stefanov et al., 2001; Hodgson et al., 2003) or for combining multiple classification results to generate a new one (Ceamanos et al., 2010; Chitroub, 2010; Zhu, 2010).

Lu & Weng (2007) reviewed methods and potential techniques to improve classification results. For land use/cover classification in a specific study area, two critical steps are: to select suitable variables from remotely sensed and ancillary data; and to select a suitable algorithm for classification. Although much research on it has been done, it is still unclear which classification procedure is suitable for a specific study area, due to different classification systems used in previous research, different kinds of remotely sensed data and derived variables, and different classification algorithms. This paper will not provide a detailed overview of land use/cover classification methods, but attempts to provide a better understanding of land use/cover classification in the moist tropical regions of the Brazilian Amazon through a comprehensive analysis of our previous experiments (Lu, 2005; Lu et al., 2003a, 2003b, 2004a, 2004b, 2007, 2008b, 2010, 2011b, 2012; Li et al., 2011, 2012). Some specific issues for improving classification performance will also be discussed. The structure of this review is as follows: brief description of the study areas and datasets used in the research; summary of land use/cover classification by incorporating spatial information into multispectral features; overview of multi-sensor/multi-resolution data fusion in improving land use/cover classification; comparative analysis of different classification algorithms; description of a hierarchical-based procedure suitable for historical remote sensing image classification; and conclusions and discussion.

Study areas and datasets used

Three study areas, located in the Brazilian Legal Amazon, were selected for this research: Altamira, in the state of Pará; Machadinho d'Oeste, in the state of Rondônia; and Lucas do Rio Verde, in the state of Mato Grosso (Figure 1). Altamira is located along the Transamazon highway (BR-230), in the state of Pará, in northern Brazil. The dominant native types of vegetation are mature moist forest and liana forest. Deforestation, since the early 1970s, has led to a complex landscape consisting of different succession stages, pasture, and agricultural lands (Moran et al., 1994; Moran & Brondizio, 1998; Li et al., 2011; Lu et al., 2011b). Machadinho d'Oeste is located in northeastern Rondônia, near the borders with the states of Amazonas and Mato Grosso. Settlement began in the early 1980s and since then land-use/cover trajectories, following deforestation, have put in place a dynamic process of forest fragmentation (Batistella et al., 2003; Lu, 2005; Lu et al., 2008a). Lucas do Rio Verde, in the state of Mato Grosso, was established in 1982 and has a relatively short history and small urban extent, but has experienced rapid urbanization and deforestation (Lu et al., 2011b). The major vegetation types include primary forest, cerrado, and limited areas of regenerating vegetation that appeared in recent years. Deforestation began in the late 1970s with the construction of the BR-163 highway and expanded, especially after the establishment of the municipality of Lucas do Rio Verde (Lu et al., 2012).

Different sensor data were used in this research, and all the satellite images were geometrically rectified into the universal transverse mercator coordinate system. Landsat and "Satellite Pour l'Observation de la Terre" (Spot) images were atmospherically calibrated into surface reflectance with the improved dark-object subtraction method (Lu et al., 2002, 2008b; Chander et al., 2009). Radar data, including Alos Palsar L-band and Radarsat C-band, were used, and speckle reduction was implemented by using filtering methods (Lu et al., 2007, 2011b). High spatial resolution images, such as Ikonos and QuickBird, were mainly used to support the selection of samples for land use/cover classification procedures.

In the Altamira study area, Landsat 5 Thematic Mapper (TM) imagery (acquired on July 2, 2008), Alos Palsar FBD (fine beam double polarization) Level 1.5 product with HH and HV polarization options (ground range, unsigned 16-bit integral number, 12.5 m pixel spacing) (Eorc, 2012) (acquired on July 2, 2009), QuickBird imagery (acquired in 2008), and field survey data (collected in 2009) were used. The Alos Palsar L-band HH and HV images were resampled to a pixel size of 10x10 m with the nearest-neighbor sampling method during image-to-image registration. For a more detailed description of image preprocessing for

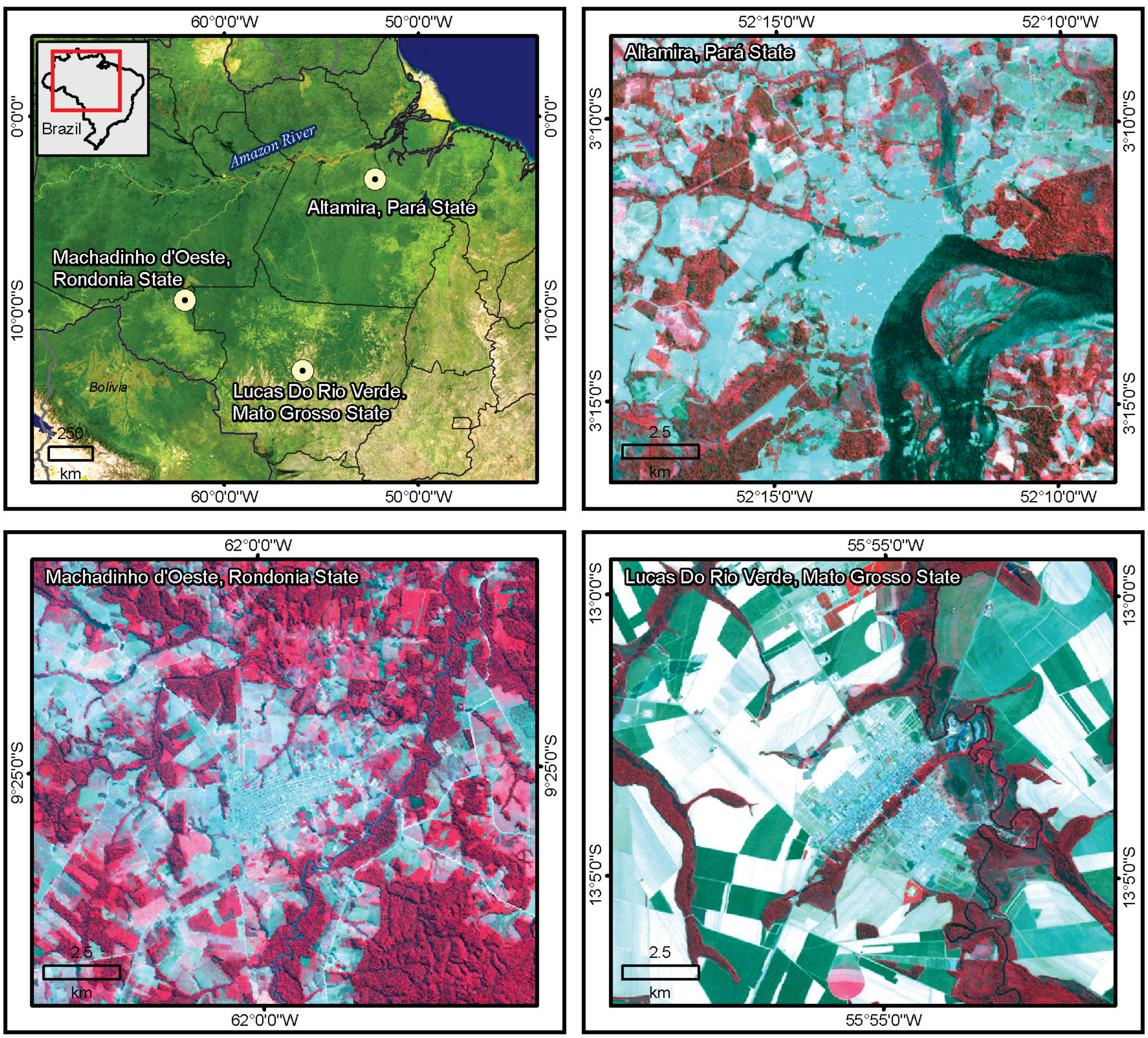

Figure 1. Three study areas in the Brazilian Amazon – Altamira, in the state of Pará; Machadinho D'Oeste, in the state of Rondônia; and Lucas do Rio Verde, in the state of Mato Grosso.

Landsat TM and Palsar L-band data in the Altamira study area see Lu et al. (2011b).

For the Machadinho d'Oeste study area, fieldwork was conducted in 1998/1999 and in 2002/2003. Satellite images– Ikonos (May 28, 2001), Radarsat-1 C-band HH (September 21, 2001), Spot HRG (high resolution geometrical) (June 26, 2003), Landsat Enhanced Thematic Mapper Plus (ETM) (August 11, 2001), and Landsat TM (July 8, 2003) were used. The Spot HRG image has five bands, covering one panchromatic band with 5 m spatial resolution, two visible (green and red) bands, one near infrared (NIR) band with 10 m spatial resolution, and one shortwave infrared (SWIR) band with 20 m spatial resolution. The Radarsat-1 C-band HH image was resampled to a pixel size of 15x15 m during the image-to-image registration. More details about image preprocessing for the Machadinho d'Oeste study area are provided in Lu et al. (2004b, 2007, 2008b).

For the Lucas do Rio Verde study area, QuickBird images (acquired in 2004 and 2008) were used in the urban-rural landscape. QuickBird imagery has four multispectral bands (blue, green, red, and near-infrared), with spatial resolution of 2.4 m, and one panchromatic band (visible wavelength) with spatial resolution of 0.6 m. In order to make full use of multispectral and panchromatic features in the QuickBird image, a wavelet-based data fusion method was used to generate new multispectral data with improved spatial resolution of 0.6 m (Lu et al., 2010). For the county scale, three Landsat 5 TM images (acquired on September 17, 2002; July 17, 2005; and May 22, 2008) were used for land use/cover classification. More details on image preprocessing for the Lucas do Rio Verde study area are provided in Lu et al. (2010, 2011b).

Land use/cover classification – from spectral signature to the combination of spectral and spatial features

Remote sensing data includes spectral, spatial, radiometric, and temporal resolution characteristics, as well as variations in polarization and angle (Althausen, 2002; Lefsky & Cohen, 2003). Most remote sensing applications, especially using medium and coarse spatial resolution images, are mainly based on spectral signatures for land use/cover classification. As spatial resolution increases, the effective use of spatial information becomes a more important research topic. The common methods for using spatial information are textures and segmentation, which are the foci of this section on the roles of spatial information in improving land use/cover classification.

Texture often refers to the pattern of variation in intensity in an image. Many texture measures have been developed and used for land use/cover classification (Haralick et al., 1973; Herold et al., 2003; Yu et al., 2006; Lu et al., 2010; Li et al., 2011). Of the many texture measures, the grey-level co-occurrence matrix (GLCM) has been extensively used for land-cover classification (Marceau et al., 1990; Lu et al., 2008b, 2011b). In this study, GLCM-based texture measures (e.g., variance, homogeneity, contrast, dissimilarity, entropy, and second moment) with different window sizes (e.g., 5x5, 9x9, 15x15, 19x19, 25x25, and 31x31) were applied to different sensor data, such as Landsat TM, Spot Panchromatic, Palsar L-band, and QuickBird images (Lu et al., 2007, 2008b, 2010; Li et al., 2011, 2012). Because many textural images are calculated with different texture measures, window sizes, and image bands, it is critical to identify the ones suitable for a given study. Therefore, separability analysis with transformed divergence, based on training sample plots of different land cover classes, is used to select potential single textural images and a combination of two or more textural images. When two or more textural images are selected, the correlation coefficient between textural images and the standard deviation of each textural image are used to identify the best combination, as described in Li et al. (2011). The selected textural images are then incorporated as extra bands into multispectral or radiometric images for land use/cover classification.

Another common method to use spatial information is based on image segmentation, i.e., partitioning of raster images into spatially continuous, disjointed and homogeneous regions, called segments, based on pixel values and locations (Blaschke et al., 2004). Pixels that have similar spectral values, which are spatially connected, are grouped in a single segment. A critical step is to develop a segmentation image, which is often based on pixel, edge, and region methods (Blaschke et al., 2004; Yu et al., 2006). In the land cover classification using Landsat TM and Palsar data in Altamira, the segmentation-based method included the following steps: image segmentation – a moving window assesses spectral similarity across space and over all input bands, and segments are defined based on user-specified similarity thresholds; creation of training sites and signature classes based on image segments; and classification of the segments (Li et al., 2011). In the study with QuickBird imagery in Lucas do Rio Verde, the major steps were: producing a segmentation image from the QuickBird multispectral one and converting the segmentation image into a vector format image, removing the segments with small areas; extracting the mean spectral value of each segment for each band, and conducting supervised classification for the mean-spectral value image (Lu et al., 2010).

Role of spatial information in land use/cover classification in Altamira

In the Altamira study area, two textural images developed with dissimilarity texture measures on Landsat red and near-infrared wavelength images and a window size of 9x9 pixels were used. Details are described in Li et al. (2011). Compared with spectral signatures, textural images have significantly different features in reflecting land use/cover types, as illustrated in Figure 2. Therefore, the incorporation of textural images and spectral signatures has the potential to improve land use/cover classification. In this study, two textural images were incorporated as extra bands into TM multispectral images for land use/cover classification with the

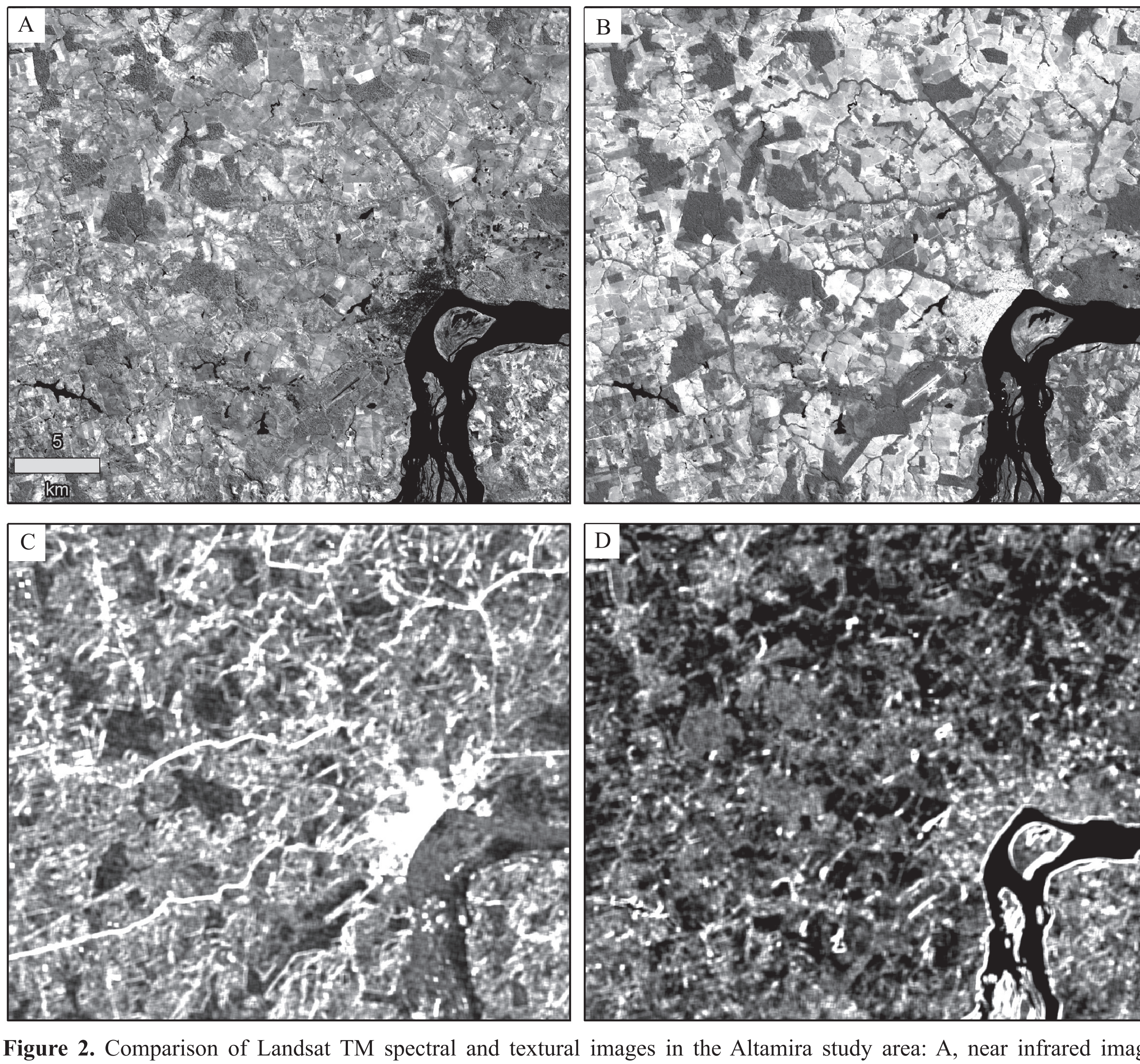

Figure 2. Comparison of Landsat TM spectral and textural images in the Altamira study area: A, near infrared image (band 4); B, shortwave infrared image (band 5); C and D, two textural images based on dissimilarity on red wavelength (band 2) and near infrared (band 4) with a window size of 9x9 pixels.

maximum likelihood classifier (MLC). For comparison, the MLC was also used to classify Landsat TM multispectral bands into a thematic map. Meanwhile, a segmentation-based classification was conducted for the TM multispectral bands (Li et al., 2011). During image classification, a total of 254 sample plots (over 3,800 pixels), covering the 11 land use/cover types (i.e., three primary forest types, three secondary succession stages, agro-pasture, and four other classes) in which each land cover type had 15–30 plots, were used as training samples. After classification, a total of 338 test sample plots from the field survey and the QuickBird image were used for accuracy assessment. The error matrix approach was used to evaluate the classification accuracy. Producer's and user's accuracy for each land cover type, as well as overall accuracy and kappa coefficient for each classified image, were calculated from the error matrix (Congalton, 1991; Foody, 2002; Congalton & Green, 2008).

The accuracy assessment results for the Altamira study area are summarized in Table 1. In comparison with the classification results based on TM multispectral bands, the incorporation of textural images into multispectral bands slightly improved overall accuracy by approximately 3%, which improved upland and flooded forests, secondary succession stages, and non-vegetated land cover classes. Even though the segmentation-based method did not significantly improve overall accuracy in this study, it did improve accuracy for some land cover types, such as upland and flooded forests. Because the large spectral variation within the same land cover class is one of factors that results in land use/cover misclassification, the use of textures or segments in this study has proven valuable for improving forest classification due to the effects of complex forest stand structures.

In another experiment in Altamira for a relatively small area with Alos Palsar L-band HH and HV images, four textural images were selected: two textural images developed from a L-band HH image with second moment and a window size of 25x25 pixels, and with contrast texture measure and a window size of 31x31 pixels; and two textural images developed from a L-band HV image with contrast and a window size of 25x25 pixels, and with second moment texture measure and a window size of 19x19 pixels (Li et al., 2012). The selected textural images, compared with the original HH or HV image (Figure 3), have considerably

Table 1. Comparison of accuracy assessment results based on different scenarios from the 2008 Landsat TM and 2009 Alos Palsar L-band images in Altamira, in the state of Pará, Brazil[(1)].

Land	2008 Landsat TM data						2009 Alos Palsar data					
cover	MLC				Segmentation based		MLC				Segmentation based method	
types	Multispectral (MS) bands		MS & textures		method on MS bands		HH & HV		HH & HV & textures		HH & HV & textures	
	PA	UA	PA	UA	PA	UA	PA	UA	PA	UA	PA	UA
Upland forest	37.0	95.2	66.7	78.3	53.7	78.4	27.3	30.0	51.5	39.5	33.3	44.0
Flooding forest	93.8	50.0	100.0	66.7	93.8	75.0	80.0	54.6	73.3	61.1	80.0	63.2
Liana forest	95.5	66.7	81.8	66.7	95.5	68.9	-	-	25.0	15.8	58.3	21.2
SS1	84.0	61.8	92.0	57.5	72.0	58.1	31.6	46.2	42.1	50.0	42.1	53.3
SS2	67.9	90.5	78.6	95.7	67.9	82.6	54.2	33.3	66.7	64.0	62.5	68.2
SS3	89.7	74.3	79.3	85.2	72.4	63.6	23.8	27.8	23.8	38.5	28.6	35.3
Agro pasture	83.3	94.8	75.8	96.2	81.8	91.5	88.5	53.5	76.9	62.5	88.5	67.7
Water	68.2	100.0	72.7	100.0	77.3	100.0	95.8	100.0	83.3	95.2	91.7	88.0
Wetland	53.9	100.0	69.2	100.0	53.9	100.0	26.7	50.0	33.3	55.6	20.0	75.0
Urban area	100.0	71.1	100.0	79.4	100.0	77.1	30.4	77.8	60.9	87.5	60.9	77.8
Burn scars	100.0	87.5	92.9	100.0	100.0	93.3	-	-	-	-	-	-
Overall accuracy	77.2		80.2		77.8		48.1		56.1		57.1	
Kappa	0.75		0.78		0.75		0.42		0.51		0.52	

[(1)]There are no burn scars in the Palsar L band data because the study area based on Palsar data is much smaller than the one based on the Landsat TM image. PA and UA, producer's and user's accuracy, respectively; mLC, maximum likelihood classifier. SS1, SS2 and SS3, initial, intermediate, and advanced succession vegetation, respectively.

different characteristics in reflecting land cover types. When compared with Landsat TM multispectral imagery, Palsar data, either HH and HV images or the derived textural images, have relatively poor visual interpretation effects, making it difficult to use them for land use/cover classification.

Based on the field survey data and the 2008 QuickBird image, a total of 220 sample plots (over 3,500 pixels), covering the ten land cover types (no burn scars, compared with the classification with Landsat TM image), each consisting of 15–30 plots, were used for image classification. The MLC was used to classify Palsar L-band HH and HV images, and to combined dataset of the HH and HV and four textural images into thematic maps. The segmentation-based method was also used to classify the combination of HH, HV, and textural images into a thematic map. In order to compare the classification results, a total of 212 test sample plots were independently selected from the field survey and from the 2008 QuickBird image, and were used for accuracy assessment of each classified image, with 12–33 plots for each land cover. Classification evaluation results are also summarized in Table 1, in comparison with the accuracy assessment results of the Landsat TM data. Overall, the classification accuracy of the Palsar L-band data was much lower than that of the Landsat TM image. Palsar L-band HH and HV images made it especially difficult to separate different vegetation types. Incorporation of textural images into Palsar L-band HH and HV images improved overall classification accuracy by approximately 8%. Almost all land cover types enhanced classification accuracies to a certain degree, but their accuracies were still much lower than those of the Landsat TM image. Figure 4 compares land use/cover classification results of the Landsat multispectral image to those of the combination of the Palsar HH, HV, and textural images. To clearly illustrate the major land use/cover distribution, upland, flooding and liana forests were merged as forest; and initial, intermediate, and advanced succession stages were merged as secondary succession (SS). This indicates that urban, forest, and succession vegetation cannot be effectively separated from the Palsar L-band due to their rough surfaces, resulting in similar high amplitude values (Figure 3). However, the segmentation-based classification method, which considered the combination of HH, HV and corresponding textural images, slightly improved overall accuracy by approximately 1%, when compared with the result obtained by using the MLC on the same data source. The segmentation-based method further improved the accuracies of flooded forest, liana forest, and agro-pasture.

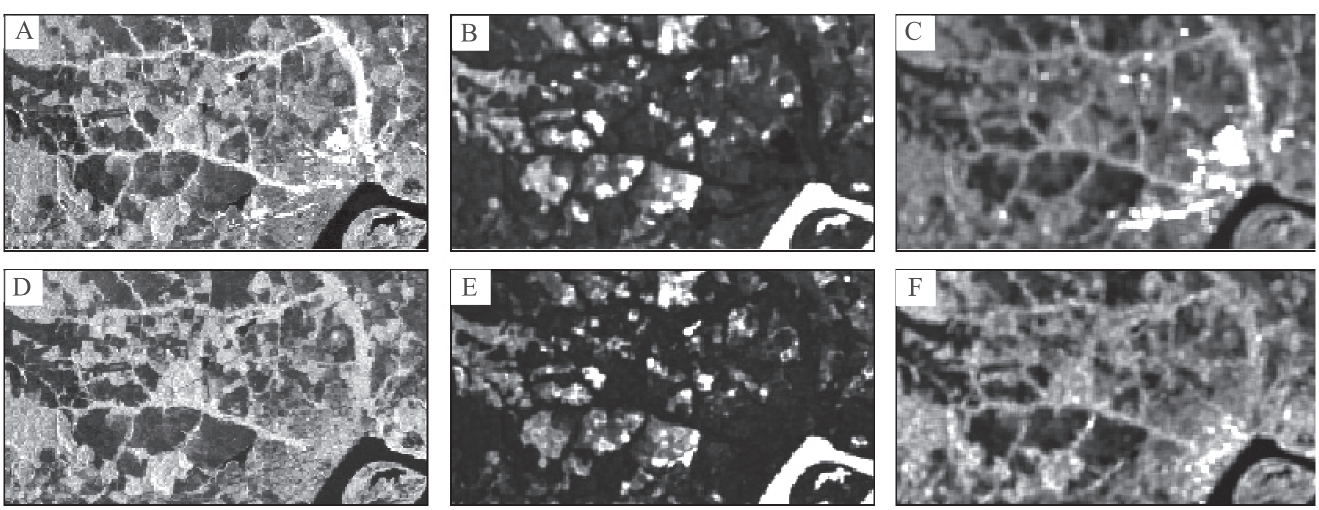

Figure 3. Comparison of Alos Palsar L band HH, HV, and derived textural images in the Altamira study area. A, B and C, L band HH, HH derived SM25, and CON31 textural images; D, E and F, L band HV, HV derived CON25, and SM19 textural images. SM25 and SM19 represent second moment with a window size of 25x25 pixels and of 19x19 pixels; CON31 and CON25 represent contrast with a window size of 31x31 pixels and of 25x25 pixels.

Role of spatial information in land use/cover classification in Machadinho d'Oeste

In the Machadinho d'Oeste study area, the 2001 Landsat ETM image was used to conduct land use/cover classification, consisting of 12 land use/cover classes. Since the ETM panchromatic band has higher spatial resolution (15 m) than ETM multispectral bands (30 m), three textural images with mean texture measure and a window size of 15x15 pixels, variance and second moment texture measures with a window size of 21x21 pixels, were selected, based on separability analysis (Lu et al., 2007). The MLC was used to classify the ETM multispectral image and the combination of ETM multispectral bands and textural images, based on the same training samples. Approximately 12–20 sample plots were selected for each class with a polygon size of 9 to 40 pixels for each plot, depending on the homogeneity of the land-cover patch. After classification, a total of 345 sample plots from the field survey in 1998/1999 and in 2002/2003 were used for accuracy assessment with the error matrix approach.

In another experiment in this study area with the 2003 Spot image for vegetation classification, two textural images were developed from the Spot panchromatic image by using entropy texture measure with a window size of 9x9 pixels and by using dissimilarity with a window size of 15x15 pixels (Lu et al., 2008b). A classification system with nine vegetation classes was designed (Lu et al., 2008b). Approximately 12–20 sample plots for each vegetation class were selected as training samples. The MLC was then used to conduct vegetation classification based on Spot multispectral bands and on the combination of Spot multispectral and textural images separately. A total of 306 test samples from the field survey in 2002/2003 and the 2001 Ikonos image were used for accuracy assessment with the error matrix approach.

The accuracy assessment results based on the 2001 Landsat ETM and the 2003 Spot images for the Machadinho d'Oeste study area are summarized in Table 2. For the 2001 ETM image, incorporation of textural images improved overall accuracy by approximately 1.8% for 12 land use/cover types, mainly for upland forest, flooding forest, and SS3. For the 2003 Spot image, incorporation of textural images improved overall accuracy by approximately 5.5% for nine vegetation types, particularly for upland open or dense forests, SS2, degraded and cultivated pastures. In comparison with ETM and Spot data, the textural images

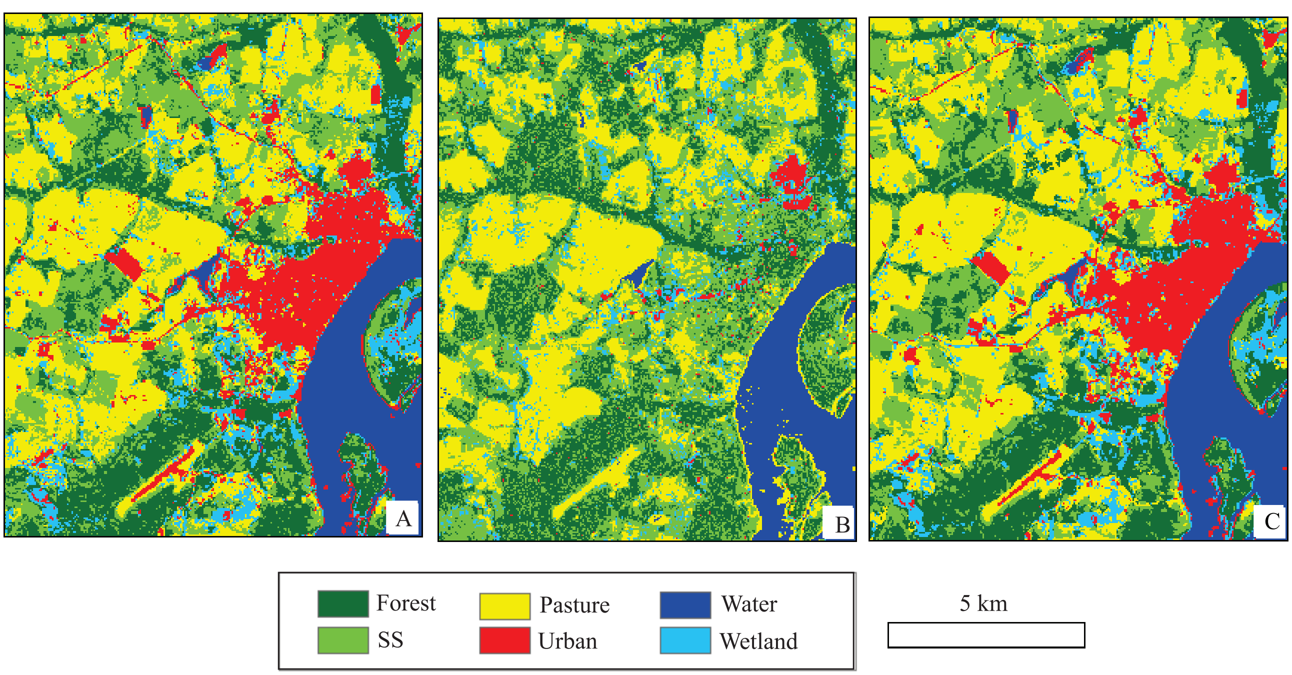

Figure 4. Comparison of classification results for the Altamira study area from different datasets: A, original TM image; B, Palsar L band data; C, TM multispectral and Palsar L band HH fusion image, with the wavelet merging technique.

from higher spatial resolution images (Spot panchromatic band with 5 m vs. ETM panchromatic band with 15 m) play a more important role in improving vegetation classification performance. Both Landsat ETM and Spot HRG data have relatively poor classification performance for secondary successional stages (i.e., SS1, SS2 and SS3) (Table 2). The main reason is that the successional stages in this study area were relatively young (less than 13 years) without clear boundaries between them (Lu, 2005; Lu et al., 2008b).

Role of spatial information in land use/cover classification in Lucas do Rio Verde

The research carried out in Altamira and Machadinho d'Oeste is based on the use of medium spatial resolution images–Landsat TM/ETM, Spot, and Alos Palsar. However, the following case study is based on the examination of a very high spatial resolution image for land use/cover classification in a complex urban-rural landscape in Lucas do Rio Verde. A QuickBird image acquired on June 20, 2008 was used, and the wavelet-merging technique was adopted to integrate QuickBird multispectral and panchromatic data into a new multispectral image with spatial resolution of 0.6 m (Lu et al., 2010). Two textural images were developed with mean and dissimilarity texture measures with a window size of 9x9 pixels on the fused QuickBird red-band image (Lu et al., 2010). In the urban landscape, different impervious surface areas, such as building roofs, roads, and parking lots, have different spectral signatures and are confused with other land covers, including bare soils, water, wetland, and crop residues, due to their similar spectral signatures (Lu et al., 2010). Therefore, different impervious surface training sample classes were selected, representing low-, medium-, and high-spectral-value impervious surfaces, dirty roads, parking lots, and shadowed impervious surface. Other land covers included upland forest, riverine forest, agroforestry, grassland/pasture, bare soils, shadows, cropped fields, water, and non-forest wetlands. At least 15 sample plots for each training class were selected, based on visual interpretation on the QuickBird false color composite. The MLC was used to classify the fused QuickBird multispectral bands and the combination of multispectral and textural images into thematic maps. The segmentation-based method was also used to classify the fused QuickBird multispectral image. Final classification results were merged into seven classes: forest, impervious surface area, pasture/grass, water, wetland, bare soils, and crop fields. A total of 300

Table 2. Comparison of accuracy assessment results with maximum likelihood classification based on the 2001 Landsat ETM and the 2003 Spot HRG data, in Machadinho d'Oeste, in the state of Rondônia, Brazil(1).

Land cover	2001 ETM MS bands		ETM MS & Pan textures		2003 Spot MS bands		Spot MS & Pan textures	
	PA	UA	PA	UA	PA	UA	PA	UA
Upland forest(2)	73.1	95.0	80.8	91.3	62.5	92.6	67.5	93.1
Upland open forest	-	-	-	-	58.3	58.3	100.0	75.0
Flooding forest	84.6	64.7	92.3	75.0	75.0	42.9	75.0	46.2
SS3	46.2	18.2	84.6	27.5	66.7	30.0	66.7	35.3
SS2	21.4	45.0	21.4	52.9	47.2	38.6	61.1	43.1
SS1	64.6	63.6	61.5	63.5	62.0	63.3	54.0	62.8
Degraded pasture	48.7	66.7	48.7	58.1	63.2	49.0	71.1	50.9
Cultivated pasture	90.9	94.3	96.4	94.6	66.0	86.8	84.0	95.5
Agroforestry	62.5	37.0	46.9	40.5	50.8	76.2	46.0	85.3
Coffee plantation	66.1	73.6	72.9	71.7	-	-	-	-
Imperviousness/bare soils	90.9	100.0	90.9	100.0	-	-	-	-
Water	100.0	84.6	100.0	78.6	-	-	-	-
Non vegetated wetland	83.3	100.0	75.0	100.0	-	-	-	-
Overall accuracy	65.2		67.0		59.2		64.7	
Kappa	0.61		0.63		0.53		0.59	

(1)PA and UA, producer's and user's accuracy, respectively; MS and Pan, multispectral bands and panchromatic band, respectively. SS1, SS2 and SS3, initial, intermediate, and advanced succession vegetation, respectively. (2)Upland dense forest for 2003 Spot MS bands and Spot MS and Pan textures.

test samples for each classification result were randomly selected for accuracy assessment with the error matrix approach.

Accuracy assessment results among different classification methods are summarized in Table 3. Compared with the classification results based on multispectral bands, incorporation of textural images and use of the segmentation-based method improved overall accuracy by 11.6% and 12.6%, respectively. Use of spatial information based on QuickBird image improved classification accuracy almost for every land cover type, which is especially valuable for forest, impervious surface, wetland, bare soils, and crop fields. Use of spatial information in the urban landscape reduced spectral variation within the same land cover classes, as well as the noise problem, which is common in per-pixel based classification methods. Crop fields were misclassified as urban or pasture/grass by the MLC (Figure 5), but this problem was significantly reduced when the segmentation-based classification method was used. This case study indicates that the proper use of spatial information is fundamental for improving land use/cover classification when very high spatial resolution images are used.

A summary of spatial information in land use/cover classification

The comparison between Tables 1, 2, and 3 shows that spatial information becomes more crucial as spatial resolution increases. When spatial resolution is around 15–30 m, as in Landsat TM and ETM images, overall accuracy by incorporating textural images into multispectral data was only slightly improved by 1.8–3%. When spatial resolution increases to 5–10 m, as in Spot HRG and Alos Palsar L-band data, overall accuracy improved by 5–8%. In particular, the role of textures from radar data is more important than those from optical sensor data in improving land use/cover classification accuracy. When spatial resolution increases as high as 0.6 m in the fused QuickBird image, the incorporation of textural images increased overall accuracy by 11.6% in an urban-rural landscape. The comparison between the segmentation-based method and the MLC indicates that the former is especially valuable for very high spatial resolution images, such as QuickBird, but much less effective for medium spatial resolution images, such as Landsat. This research implies the importance of incorporating spatial information into multispectral bands to improve land use/cover classification. As spatial resolution increases, the spectral variation within the same land cover is enlarged. Use of texture measures or segmentation can reduce spectral variation and improve classification accuracy.

Land use/cover classification – from individual sensor data to the integration of multi-resolution/multi-sensor data

Data fusion is often used for the integration of multi-sensor or multi-resolution data to enhance visual interpretation and to improve the performance of quantitative analysis (Klonus & Ehlers, 2007; Lu & Weng, 2007). Many data fusion methods,

Table 3. Comparison of accuracy assessment results from the 2008 QuickBird image in Lucas do Rio Verde, in the state of Mato Grosso, Brazil(1).

Land cover	Maximum likelihood classifier				Segmentation-based method on MS image	
	Multispectral (MS) image		Combination of MS & texture			
	PA	UA	PA	UA	PA	UA
Forest	92.5	71.0	95.1	89.2	90.6	90.3
Imperviousness	95.1	76.5	90.9	85.1	87.8	92.3
Pasture/grass	75.0	62.3	74.5	77.8	75.0	71.7
Water	71.0	100.0	80.0	100.0	96.8	100.0
Wetland	31.0	52.9	88.9	72.7	100.0	82.9
Bare soils	69.7	82.1	87.1	93.1	93.9	86.1
Crop fields	75.4	86.7	89.9	91.2	84.1	95.1
Overall accuracy	75.7		87.3		88.3	
Kappa	0.71		0.85		0.86	

(1)PA and UA, producer's and user's accuracy, respectively.

such as principal component analysis (PCA), the wavelet-merging technique, intensity-hue-saturation, and Ehlers fusion, have been developed to integrate spectral and spatial information (Pohl & Van Genderen, 1998; Klonus & Ehlers, 2007; Dong et al., 2009; Ceamanos et al., 2010; Ehlers et al., 2010; Zhang, 2010). The major methods have been reviewed by Pohl & Van Genderen (1998) and Zhang (2010). Of the many fusion techniques, wavelet-based merging has been regarded as a valuable method in improving land use/cover classification (Lu et al., 2007, 2008b), and therefore, it is used in this research.

In the wavelet-based method, an image can be decomposed into high- and low-frequency components. The low-frequency component represents the lower spatial resolution image and the high-frequency one represents the higher spatial resolution image, containing greater spatial details. In general, the high spatial resolution image is a single band, such as the Palsar L-band, Radarsat C-band, Landsat ETM and Spot panchromatic band. The low spatial resolution image is from a multispectral one, such as the Landsat TM/ETM or Spot multispectral images used. Since the substitution of the low spatial resolution image is done by using multispectral data, it is necessary to select a single image from the multispectral image to replace the low-frequency image from the wavelet transform. Therefore, PCA is often used to convert the multispectral bands to a new dataset, and the first component (PC1) from the multispectral bands is used to replace the low-frequency image, because PC1 contains most of the information. The inverse wavelet transform is then used to convert the replaced dataset into a new multispectral one, which incorporates both multispectral and panchromatic or radar information, with improved spatial resolution (Lu et al., 2011b). The wavelet theory has been discussed in detail in the literature (Chibani, 2006; Amolins et al., 2007; Hong & Zhang, 2008).

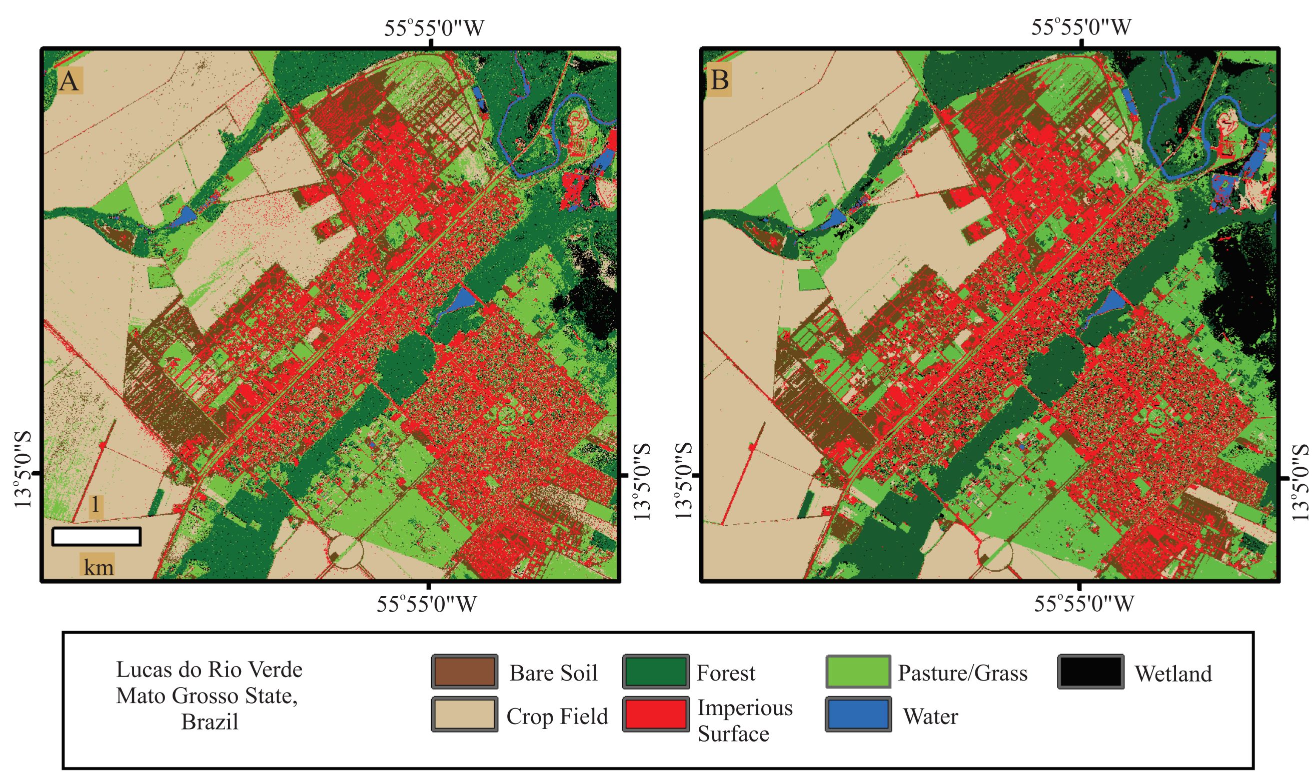

Figure 5. Comparison of classified images for the Lucas do Rio Verde study area based on the 2008 QuickBird image by using the: A, maximum likelihood classifier; and B, segmentation based method.

Landsat TM and radar data fusion in Altamira

In the relatively small study area in Altamira, the 2008 Landsat TM multispectral and the Palsar L-band HH images were used to generate a new fused multispectral image with spatial resolution of 15 m by the wavelet-merging technique (Lu et al., 2011b). The same training and test samples, as described in section 3.1 for Palsar data classification, were used. The MLC was then used to classify the fused and the TM multispectral images into thematic maps with a classification system of ten land use/cover classes. The classification result based on the TM multispectral and Palsar L-band HH data fusion was illustrated in Figure 4. Accuracy assessment results indicate that data fusion with the wavelet-merging technique improved overall accuracy by approximately 4.8% (Table 4). Data fusion was especially valuable for improving the accuracy of successional vegetation classes, upland and liana forests, and agro-pasture. Since the long wavelength radar data can penetrate the forest canopy into a certain depth to capture more information about understory and non-photosynthetic vegetation (e.g., branch and stem) (Kasischke et al., 1997), incorporation of radar L-band data into multispectral image may increase spectral information, improving spatial resolution (from 30 m in TM multispectral image to 15 m in fusion image) and classification performance.

Table 4. Comparison of accuracy assessment results with maximum likelihood classification from the 2008 Landsat TM image and the fusion image based on TM and Palsar L band HH images in Altamira, in the state of Pará, Brazil(1).

Land cover	TM multispectral (MS) bands		Fusion of TM MS & Palsar L-HH	
	PA	UA	PA	UA
Upland forest	69.7	88.5	75.8	89.3
Flooding forest	93.3	73.7	93.3	70.0
Liana forest	83.3	71.4	91.7	84.6
SS1	57.9	57.9	79.0	71.4
SS2	87.5	75.0	87.5	91.3
SS3	85.7	85.7	90.5	86.4
Agro pasture	73.1	82.6	80.8	91.3
Water	87.5	100.0	87.5	100.0
Wetland	80.0	92.3	80.0	100.0
Urban area	100.0	82.1	100.0	79.3
Overall accuracy	81.1		85.9	
Kappa	0.79		0.84	

(1)PA and UA, producer's and user's accuracy, respectively; SS1, SS2 and SS3, initial, intermediate, and advanced succession vegetation, respectively. The classification results in Table 4, considering TM multispectral bands, differ from those in Table 1 because of the different size of the study area and the number of land use/cover classes.

Multi-sensor/multi-resolution data fusion in Machadinho d'Oeste

In the Machadinho d'Oeste study area, a 2001 Landsat ETM and a Radarsat-1 C-band HH imagery were used for land use/cover classification (Lu et al., 2007). Because the Landsat ETM image has a panchromatic band with 15 m spatial resolution, the wavelet-based merging technique was used to merge the ETM multispectral bands and the panchromatic band, as well as to merge ETM multispectral bands and the Radarsat-1 C-band HH image into new datasets with spatial resolution of 15 m. Approximately 12–20 sample plots were selected for each class with a polygon size of 9 to 40 pixels for each plot, depending on the homogeneity of the land-cover patch. The MLC was then used to separately classify the fused images and the ETM multispectral image into thematic maps with a classification system of 12 land use/cover classes. After classification, a total of 345 sample plots were used for accuracy assessment with the error matrix approach.

Accuracy assessment results for three Landsat ETM-based data scenarios are summarized in Table 5. In comparison with Table 4, where data fusion of TM multispectral and Palsar L-band data improved overall classification accuracy by 4.8%, the results in Table 5 indicate that data fusion based on ETM multispectral bands and the panchromatic band or Radarsat-1 C-band data slightly reduced classification accuracy. When compared to the results from the ETM multispectral image, the ETM multispectral and panchromatic data fusion reduced overall accuracy by 4.3%. Most of the land cover types, except for SS3, had reduced classification accuracies. However, although the ETM multispectral and Radarsat C-band HH data fusion slightly reduced overall accuracy by 0.6%, this fusion image did improve classification accuracies for upland forest, lowland forest, and SS3 classes, implying that incorporation of radar information into multispectral bands is valuable to improve vegetation classes having complex forest stand structure. Because the ETM panchromatic band and the multispectral bands have similar spectral features, the data fusion of ETM multispectral and panchromatic data cannot increase the spectral information. The improved spatial resolution in this fusion image is useful for visual interpretation, but not helpful for vegetation classification due to the increased spectral variation, reducing the classification accuracy. In contrast, Radarsat C-band data represents different land cover features as Landsat multispectral bands. Therefore, the integration of the C-band HH image into the multispectral bands improved the spectral information in the fusion image, besides spatial resolution. Because radar data can penetrate forest canopy to a certain depth to capture more information about vegetation stand structure, the fusion of radar and multispectral data improved vegetation classification, as confirmed in this study.

In another experiment in the Machadinho d'Oeste study area, based on the 2003 Landsat TM and Spot HRG images, the wavelet-merging technique was used to combine Spot multispectral bands and the panchromatic band, and the TM multispectral and Spot panchromatic band into new datasets with spatial resolution of 5 m (Lu et al., 2008b). Training samples selected from the 2002/2003 field survey and the 2001 Ikonos data were used to classify the multispectral bands and fusion images into thematic images, respectively, by using the MLC, which was focused on nine vegetation types (Lu et al., 2008b). Overall, data fusion based on Spot multispectral bands and panchromatic band improved overall accuracy by 2.6% in Machadinho d'Oeste, but data fusion based on TM multispectral bands and the Spot panchromatic band reduced overall accuracy by 4.9% (Table 6). The Spot multispectral and panchromatic data fusion mainly improved the classification accuracies of upland open/dense forests, flooding forest, agroforestry, and degraded/cultivated pasture classes, but reduced classification accuracies of intermediate and advanced succession stages. In contrast, comparing the results from TM multispectral image, the data fusion based on TM multispectral and Spot panchromatic data reduced classification accuracies of most vegetation classes, except upland dense forest and intermediate succession. For some vegetation types, such as upland dense and flooding forests, having complex forest stand structure, the Landsat TM image with relatively coarse spatial resolution (i.e., 30 m) can provide better classification accuracy than the Spot multispectral image with higher spatial resolution (i.e., 10 m) (Table 6). However, for most of the vegetation classes having relatively simple stand structure, such as different succession stages, the Spot image provided better classification than the TM image.

Table 5. Comparison of accuracy assessment results with maximum likelihood classification, based on the 2001 Landsat ETM, Radarsat C-band HH, and fusion images, in Machadinho d'Oeste, in the state of Rondônia, Brazil(1).

Land cover	Landsat ETM MS image		Fusion of ETM MS & Pan		Fusion of ETM MS and C-HH	
	PA	UA	PA	UA	PA	UA
Upland forest	73.1	95.0	76.9	90.9	84.6	95.7
Lowland forest	84.6	64.7	84.6	61.1	92.3	80.0
SS3	46.2	18.2	69.2	22.5	76.9	25.6
SS2	21.4	45.0	21.4	36.0	26.2	47.8
SS1	64.6	63.6	53.9	61.4	55.4	61.0
Degraded pasture	48.7	66.7	40.5	53.6	46.0	58.6
Cultivated pasture	90.9	94.3	89.1	94.2	90.9	96.2
Agroforestry	62.5	37.0	53.1	34.0	56.3	36.0
Coffee plantation	66.1	73.6	57.6	68.0	62.7	71.2
Infrastructure	90.9	100.0	90.9	90.9	90.9	90.9
Water	100.0	84.6	100.0	78.6	100.0	78.6
Non-vegetated lowland	83.3	100.0	75.0	100.0	75.0	100.0
Overall accuracy	65.2		60.9		64.6	
Kappa	0.61		0.56		0.60	

(1)PA and UA, producer's and user's accuracy, respectively; MS and Pan, multispectral bands and panchromatic band, respectively; SS1, SS2 and SS3, initial, intermediate, and advanced succession vegetation, respectively; C-HH, Radarsat C-band HH image.

A summary of multi-sensor/multi-resolution data fusion in land use/cover classification

A comparative analysis of accuracy assessment results on different data fusion scenarios (Tables 4, 5, and 6) indicates that data fusion based on multi-resolution of optical sensor data cannot guarantee the improvement of land use/cover classification accuracy, although data fusion did improve visual interpretation performance by increasing spatial resolution. The fusion results based on the TM multispectral band and Spot panchromatic band and based on ETM multispectral bands and the panchromatic band reduced overall accuracy by 4.3–4.9%, compared with the results based on corresponding multispectral bands. The accuracy reduction may imply that the incorporation of the panchromatic band cannot increase the spectral information in the fused image, except by improving spatial information. Even though increased spatial resolution is helpful in visual interpretation, the increased spectral variation within the same land cover type may reduce the classification accuracy, mainly for forest types. However, incorporation of radar data, especially L-band data, into multispectral image through data fusion techniques is valuable for improving forest classification. Incorporation of Palsar L-band data into TM multispectral bands increased overall accuracy by 4.7%, implying the importance of selecting suitable data sources in data fusion procedure.

Land use/cover classification – from parametric to nonparametric classification algorithms

Classification algorithms can be parametric and nonparametric. Nonparametric algorithms have received increasing attention because different spectral datasets or the combination of remote sensing and ancillary data are used in the classification procedure (Lu & Weng, 2007). Various classification methods, such as artificial neural network (ANN), decision tree, fuzzy-set, support vector machine (SVM), and expert systems are available (Tso & Mather, 2001; Franklin & Wulder, 2002; Lu & Weng, 2007), but one critical issue is to select a suitable classification algorithm for a specific study area or purpose. In this research, six classification algorithms – MLC, classification tree analysis (CTA), Fuzzy Artmap (a neural network method), K-nearest neighbor (KNN), object-based classification (OBC), and SVM – were examined based on Landsat TM multispectral bands and Palsar L-band data.

The MLC is the most common parametric classifier, assuming normal or near normal spectral distribution for each feature of interest. This classifier is based on the probability that a pixel belongs to a particular class and takes the variability of classes into account by using the covariance matrix (Lillesand & Kiefer, 2000; Jensen, 2005). However, the parametric algorithms are often

Table 6. Comparison of accuracy assessment results with maximum likelihood classification, based on the 2003 Landsat TM, Spot HRG, and fusion images, in Machadinho d'Oeste, in the state of Rondônia, Brazil[(1)].

Land cover	Spot HRG data				TM and Spot PAN			
	Spot MS bands		Fusion of Spot MS & PAN		Fusion of TM MS & Spot PAN		TM MS bands	
	PA	UA	PA	UA	PA	UA	PA	UA
Upland dense forest	62.5	92.6	75.0	96.8	85.0	91.9	82.5	91.7
Upland open forest	58.3	58.3	66.7	72.7	25.0	13.6	83.3	31.3
Flooding forest	75.0	42.9	87.5	50.0	87.5	41.2	87.5	58.3
SS3	66.7	30.0	55.6	20.8	11.1	7.1	33.3	20.0
SS2	47.2	38.6	41.7	35.7	25.0	25.0	11.1	23.5
SS1	62.0	63.3	62.0	66.0	66.0	56.9	68.0	51.5
Degraded pasture	63.2	49.0	68.4	55.3	42.1	48.5	57.9	51.2
Cultivated pasture	66.0	86.8	66.0	91.7	66.0	86.8	66.0	89.2
Agroforestry	50.8	76.2	54.0	81.0	41.3	70.3	49.2	75.6
Overall accuracy	59.2		61.8		52.9		57.8	
Kappa	0.53		0.56		0.46		0.52	

[(1)]PA and UA, producer's and user's accuracy, respectively; MS and Pan, multispectral bands and panchromatic band, respectively; SS1, SS2 and SS3, initial, intermediate, and advanced succession vegetation, respectively.

criticized due to the requirement of normal distribution, because this assumption is often violated, especially when multi-source data are used. Nonparametric algorithms do not have this requirement and have more advantages than traditional parametric classification algorithms (Pal & Mather, 2003; Lu et al., 2004b).

CTA is a nonparametric statistical machine learning algorithm that has the advantages of being distribution-free and easy to interpret over traditional supervised classifiers, and, therefore, has received increasing attention in remote sensing classification (Miller & Franklin, 2002; Zambon et al., 2006; Elnaggar & Noller, 2010). Fuzzy Artmap is one of the neural network classification methods that synthesize fuzzy logic and adaptive resonance theory (ART) models. Fuzzy Artmap network consists of four layers of neurons: input, category, mapfield, and output layers (Carpenter et al., 1992; Mannan et al., 1998). When using the Artmap algorithm, it is critical to identify optimal parameters, which is often very time-consuming. KNN is one of the simplest, but widely used, supervised learning algorithms (Franco-Lopez et al., 2001; Maselli et al., 2005; McRoberts & Tomppo, 2007), based on the minimum distance from image pixels to the training samples to determine the K-nearest neighbors. Selection of a suitable K value is crucial for a successful classification (Franco-Lopez et al., 2001; Tomppo & Halme, 2004) because it may affect the assignment of pixels to a class. OBC provides an alternative for classifying remotely-sensed images into a thematic map based on segments in comparison to the traditional per pixel-based classification methods (Yu et al., 2006; Blaschke, 2010). The SVM is a relatively new supervised classifier, but has gained great attention in recent years (Camps-Valls et al., 2008; Camps-Valls & Bruzzone, 2009; Perumal & Bhaskaran, 2009; Tuia et al., 2011). A recent paper by Mountrakis et al. (2011) provided a detailed review of the SVM in remote sensing field.

The 2008 Landsat TM image and 2009 Palsar L-band HH, HV, and textural images (Lu et al., 2011b) were used for land use/cover classification in the Altamira study area. In order to compare the classification capabilities among different classification algorithms, it is essential to use the same training sample plots and images, and independent test samples for evaluation of the classified results. In this research, a total of 432 sample plots were collected from the field survey in 2009 and from the 2008 QuickBird image. Of the sample plots, 220 were used as training sample plots for image classification and another 212 were used as test sample plots for accuracy assessment. The error matrix approach was used to evaluate the classified results from each classification algorithm based on both Landsat TM and Palsar L-band data.

For individual TM or Palsar data, selection of a suitable classification algorithm for land use/cover classification is important, but no single algorithm is best for each land cover type (Table 7). For example, if the classification result with the MLC, based on the Landsat TM multispectral image, is used as a benchmark, CTA, KNN, and OBC slightly improve overall accuracy, but Artmap and SVM slightly decrease overall accuracy. Examining individual classes, CTA mainly improved upland forest, initial succession stage, agro-pasture, water, and urban area; KNN improved upland forest, initial succession stage, water, and urban area; OBC improved intermediate and advanced successional stages, and water; whereas Artmap and SVM improved non-vegetation land covers. Comparing the results from Palsar L-band data with those from Landsat TM multispectral bands, Palsar data have much lower classification performance than Landsat, no matter which classification algorithms were used. In the classification image from PALSAR data, urban area was significantly underestimated, while flooded forest was greatly overestimated (Figure 6). Urban area was misclassified as upland forest and liana forest. Palsar data provided overall accuracy of only 47.6–59.4%, compared with 78.3–84.9% from the Landsat image (Table 7). Based on the classification results from Palsar data, CTA and Artmap provided relatively better performance than the others. In particular, CTA and Artmap provided good performance for upland forest, flooding forest, agro-pasture, and water, but Palsar data seemed difficult to classify liana forest, different successional vegetation stages, and wetland, no matter which classification algorithms were used. Based on the classification accuracy, image processing time, and the analyst's involvement in the classification procedure, MLC and CTA were recommended methods for this type of study. This research indicates that different classification algorithms have their own merits in land use/cover classification, which is also proven in previous research (Michelson et al., 2000; Pal & Mather, 2003, 2004; Lu et al., 2004b; Rogan et al., 2008; Li et al., 2011).

Land use/cover classification – from traditionally supervised classification methods to a hierarchical-based classification method

Although many classification methods are available, as summarized in Lu & Weng (2007), they require representative training samples to implement image classification. For historical remote-sensing data, land-use/cover classification is often difficult due to the lack of sufficient training samples that can be used for image classification. With free access and relatively long history of data availability, the application of Landsat images has been used to develop time series land use/cover datasets (Huang et al., 2010; Thomas et al., 2011). In this case study, a hierarchical-based classification method was used, consisting of stratification and cluster analysis for land use/cover classification in the municipality of Lucas do Rio Verde, based on the 2002, 2005, and 2008 Landsat 5 TM images (Lu et al., 2012).

Previous research has shown the difficulty in separating impervious surfaces from other land-use/cover types (e.g., bare soils, crop residues, and wetland) based on Landsat multispectral images (Lu

Table 7. Comparison of accuracy assessment results from different classification algorithms based on Landsat TM multispectral data and Alos Palsar L band data[1].

Land cover	MLC		CTA		Artmap		KNN		OBC		SVM	
types	PA	UA	PA	UA	PA	UA	PA	UA	PA	UA	PA	UA
						Landsat TM multispectral bands						
Upland forest	69.7	88.5	90.9	85.7	90.9	65.2	72.7	92.3	66.7	88.0	87.9	65.9
Flooding forest	93.3	73.7	86.7	72.2	73.3	64.7	80.0	70.6	86.7	68.4	86.7	81.3
Liana forest	83.3	71.4	75.0	81.8	58.3	100.0	83.3	58.8	83.3	71.4	50.0	100.0
SS1	57.9	57.9	68.4	59.1	52.6	71.4	63.2	57.1	57.9	55.0	47.4	53.0
SS2	87.5	75.0	75.0	78.3	79.2	70.4	83.3	83.3	91.7	81.5	62.5	83.3
SS3	85.7	85.7	81.0	94.4	33.3	63.6	95.2	74.1	90.5	86.4	61.9	56.5
Agro-pasture	73.1	82.6	76.9	87.0	88.5	82.1	69.2	81.8	69.2	81.8	73.1	73.1
Water	87.5	100.0	100.0	100.0	100.0	100.0	100.0	100.0	95.8	100.0	100.0	100.0
Wetland	80.0	92.3	86.7	86.7	100.0	100.0	73.3	100.0	80.0	92.3	100.0	100.0
Urban area	100.0	82.1	100.0	100.0	100.0	100.0	100.0	100.0	100.0	85.2	100.0	100.0
OCA	81.1		84.9		79.7		82.1		81.6		78.3	
OKC	0.79		0.83		0.77		0.80		0.79		0.76	
						Alos Palsar L band HH, HV, and corresponding textural images						
Upland forest	51.5	39.5	81.8	50.0	75.8	39.7	21.2	33.3	33.3	44.0	84.9	40.0
Flooding forest	73.3	61.1	80.0	60.0	80.0	70.6	73.3	52.4	80.0	63.2	80.0	54.5
Liana forest	25.0	15.8	16.7	25.0	16.7	100.0	25.0	14.3	58.3	21.2		
SS1	42.1	50.0	31.6	66.7	26.3	55.6	36.8	46.7	42.1	53.3	31.6	85.7
SS2	66.7	64.0	58.3	77.8	45.8	64.7	54.2	32.5	62.5	68.2	37.5	60.0
SS3	23.8	38.5	14.3	25.0	23.8	38.5	19.1	26.7	28.6	35.3	14.3	33.3
Agro-pasture	76.9	62.5	73.1	65.5	88.5	63.9	76.9	60.6	88.5	67.7	96.2	61.0
Water	83.3	95.2	95.8	92.0	100.0	92.3	95.8	100.0	91.7	88.0	95.8	88.5
Wetland	33.3	55.6	20.0	33.3	33.3	62.5	33.3	41.7	20.0	75.0	13.3	50.0
Urban area	60.9	87.5	73.9	60.7	60.9	66.7	34.8	72.7	60.9	77.8	52.2	66.7
OCA	56.1		59.4		59.4		47.6		57.1		56.6	
OKC	0.51		0.54		0.54		0.42		0.52		0.51	

[1]MLC, maximum likelihood classifier; CTA, classification tree analysis; Artmap, a neural network classification method that synthesizes fuzzy logic and adaptive resonance theory (ART) models; KNN, K-nearest neighbor; OBC, object-based classification; and SVM, support vector machine. PA, UA, OCA and OKC, producer's accuracy, user's accuracy, overall classification accuracy, and overall kappa coefficient, respectively. SS1, SS2 and SS3, initial, intermediate, and advanced succession vegetation, respectively.

et al., 2011c). Therefore, a hybrid method consisting of thresholding, cluster analysis, and manual editing was used to map impervious surface distribution (Lu et al., 2011c). Primary forest mapping was then conducted with the combination of thresholding on the normalized difference vegetation index (NDVI)

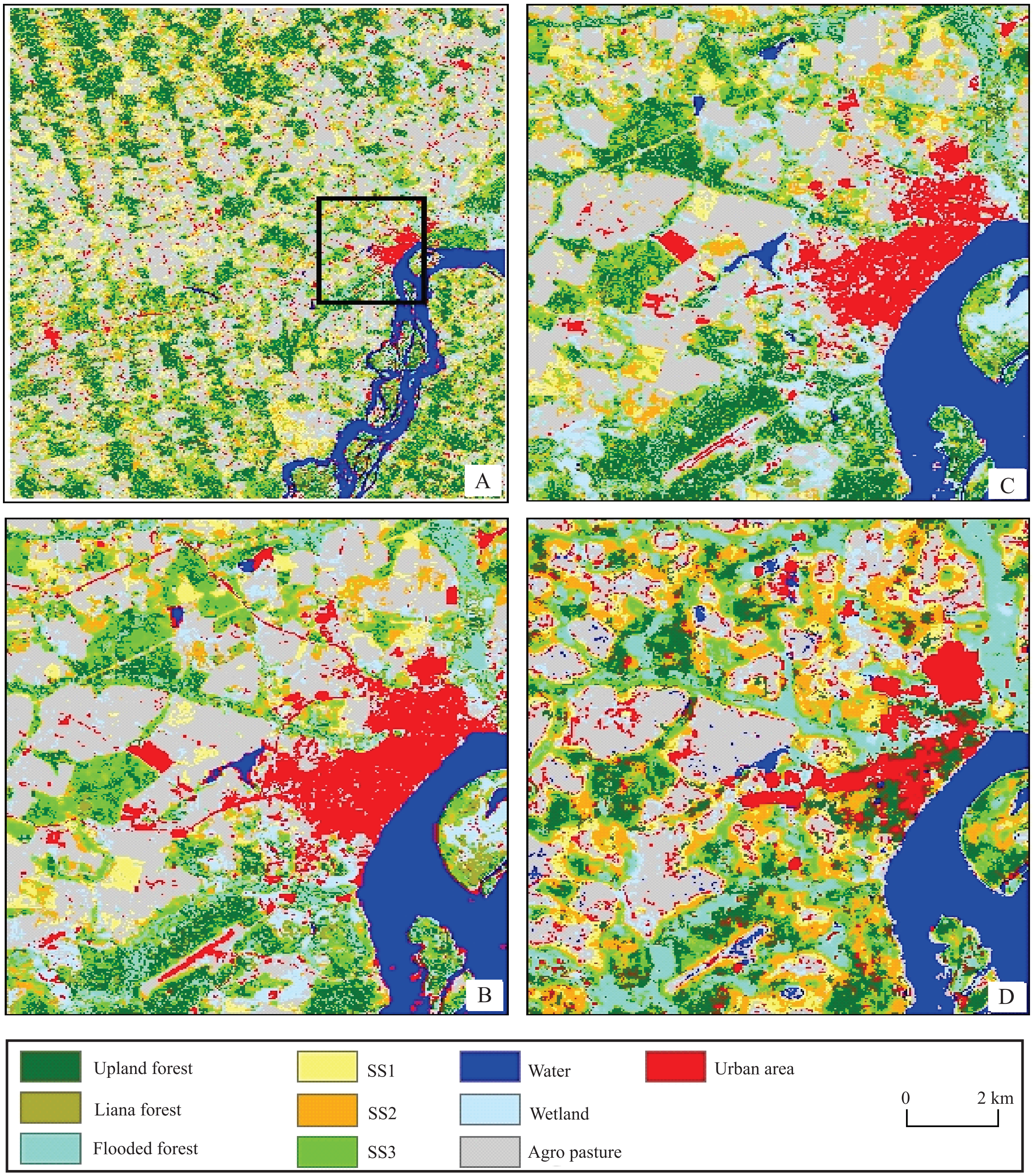

Figure 6. Comparison of classification results in the Altamira study area with maximum likelihood classification on the Landsat TM image for the entire study area (A); enlarged area for the black box in image a (B); classification tree analysis based on the Landsat TM image (C); and classification tree analysis based on the Palsar L band HH, HV, and corresponding textural images (D).

image and cluster analysis (Lu et al., 2011a). After masking impervious surfaces and forest classes from the Landsat multispectral bands, the remaining land-use/cover classes included cerrado, regenerating vegetation (e.g., plantation), agricultural land, pasture, water, and wetland. Cluster analysis was then used to classify the spectral signatures of remaining pixels into 50 clusters, and the analyst merged the clusters into cerrado, regenerating vegetation, agro-pasture, water/wetland, and mixed class (confused land covers). The mixed class was eventually classified through an iterative process of masking, cluster analysis, and recoding, that is: masking out all classified land use/cover classes and leaving only the mixed pixels; using cluster analysis to classify spectral signatures of the mixed pixels into 30 clusters; merging each cluster into one of the land use/cover classes; and recoding the merged clusters into the same labels as the land use/cover classification system (Lu et al., 2012). During the unsupervised classification, field survey data collected in 2009 and the 2008 QuickBird image were used to assist the cluster-merging process.

Landsat TM images acquired in 2002, 2005, and 2008, two QuickBird images acquired in 2004 and 2008, and some field survey data collected in 2009 were used in this research. After three dates of Landsat TM images were classified independently into thematic maps, consisting of six land use/cover classes (i.e., forest, cerrado, agro-pasture, regenerating vegetation, water/wetland, and impervious surface area), a stratified random sampling method was used to select 300 sample plots for accuracy assessment of each classified image for 2002, 2005, and 2008 in order to independently develop each error matrix. The hierarchical-based classification method provides overall accuracy of over 93% for each classified image, implying the feasibility and capability of this method in land use/cover classification, even when training samples are not available for historical Landsat TM images (Table 8). Most of the study area was occupied by agro-pasture, with limited areas of cerrado, regenerating vegetation, and impervious surfaces (Figure 7).

This research indicates that the hierarchical-based classification method avoids the dilemma of the lack of training samples for historical remote-sensing data and made full use of the analyst's experience and knowledge for accurately mapping land-use/cover distribution (Lu et al., 2012).

State of the art and the way forward

Roles of spatial features in land use/cover classification

Traditional supervised classification is often based on spectral signatures, ignoring rich spatial information inherent in remote sensing data, especially high spatial resolution images. Even though spatial features have long been regarded as an important way of improving land use/cover classification, they have not been extensively applied in practice. The main reasons may include the limitation of spatial resolution in available remotely sensed imagery in the 1980s and 1990s, since high spatial resolution images, such as Ikonos and QuickBird, were mainly available after 2000; and the lack of standards to guide the identification of suitable methods for use of spatial characteristics. Although many texture measures have been developed, identifying suitable textures for a specific study requires significant time in image processing and determination of appropriate parameters for use in texture image creation. In addition, one texture is good for some land cover types, but may not be for others depending on patch size of the land cover types. The appropriate texture image for use is often site dependent because of different landscape features, such as the variety of land cover types and patch sizes. This is often the case when selecting the appropriate moving window sizes for use in analysis.

Another method for using spatial information is segmentation-based, used to create isolated objects so that each object shares a homogeneous spectral response.

Table 8. Comparison of accuracy assessment results by using the hierarchical-based classification method on the 2002, 2005, and 2008 Landsat 5 TM images[1].

Land use/cover	TM 2002		TM 2005		TM 2008	
	PA	UA	PA	UA	PA	UA
Forest	91.4	96.4	89.1	94.2	94.4	100.0
Cerrado	81.8	87.8	80.9	82.9	80.0	87.8
Agro-pasture	98.2	97.3	96.5	974	98.2	94.7
Regenerating vegetation	100.0	84.4	96.7	93.5	96.3	81.2
Water/wetland	90.3	93.3	93.5	96.7	93.7	100.0
Imperviousness	90.0	87.1	100.0	83.9	93.9	93.9
Overall accuracy	93.0		93.0		93.7	
Kappa	0.91		0.91		0.92	

[1]PA and UA, producer's and user's accuracy, respectively.

These objects may better represent the landscape than the original pixels. During the production of the segmentation image, it is important to identify suitable thresholds for edge detection and to determine the difference between neighboring segments. The selection of the thresholds seems subjective; mainly depending on the analyst's experience and on the characteristics of land covers in the study area. No thresholds are optimal for all different land covers due to the complexity of the landscapes under investigation. However, the segmentation-based method is valuable for very high spatial resolution images than for medium spatial resolution images, as shown in this research.

Roles of multi-sensor/multi-resolution data fusion in land use/cover classification

Many fusion techniques are developed for improving visual interpretation based on multi-resolution data with optical sensors (Ehlers et al., 2010). This improvement of spatial resolution is helpful for the sites with relatively small patches of land cover types, mainly in urban landscapes. However, due to the complex stand structure in vegetation types, especially for primary forest and advanced succession, increased spatial resolution may enlarge the spectral variation within the same vegetation types, reducing the classification accuracy. There is a tradeoff between the patch size of land covers and the spectral variation caused by improved spatial resolution. Different data fusion methods have different capabilities in preserving the spectral fidelity while improving spatial resolutions (Lu et al., 2011b). It is vital to understand the role of a specific data fusion method in enhancing particular land cover types. For visual interpretation, data fusion of the same sensor data, such as ETM, Spot, and QuickBird, having multispectral and panchromatic data, can effectively improve spatial resolution while preserving spectral features, but may not add much information for quantitative analysis, such as land use/cover classification, because of their similar spectral features. In contrast, data fusion between optical and radar data may be not suitable for visual interpretation because of the differences in reflecting land surface features, but can incorporate new features from radar data into multispectral data, improving land use/cover classification performance, especially vegetation types, as confirmed in this research. More research should be done on the development of new data fusion methods to effectively incorporate optical multispectral bands and radar data for improving quantitative analysis performance.

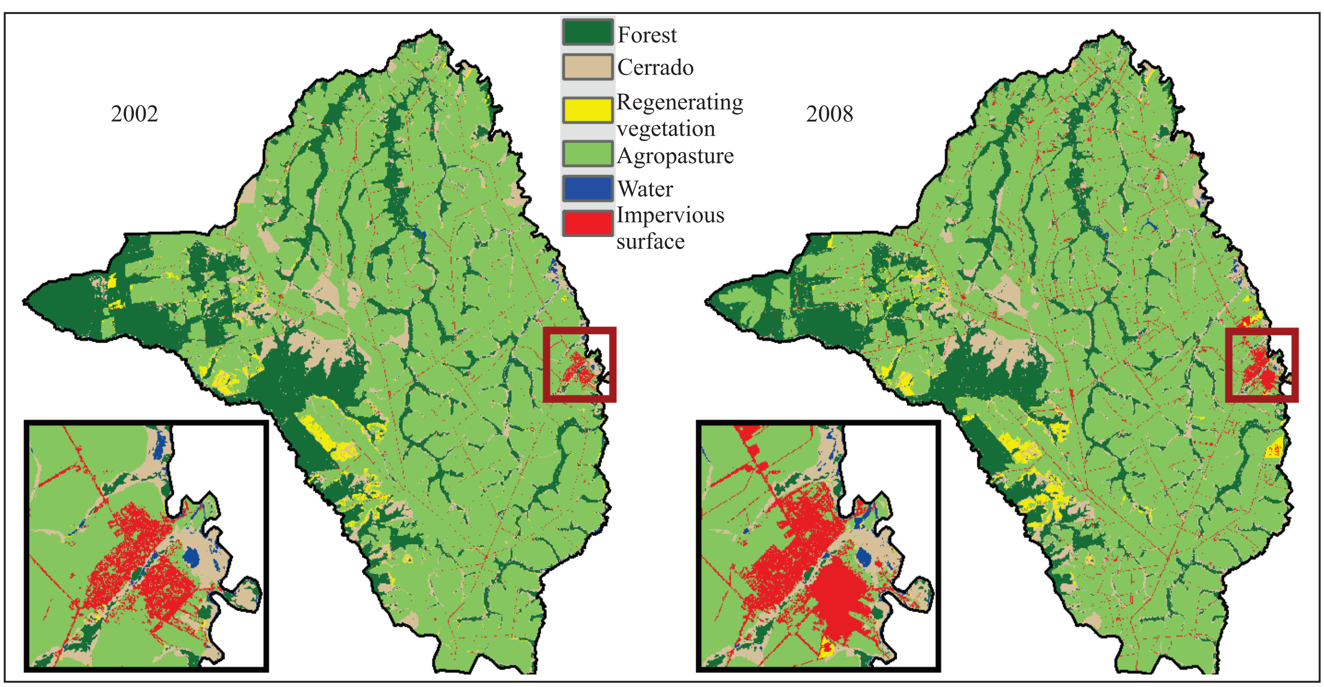

Figure 7. Comparison of classification results for the municipality of Lucas do Rio Verde, based on the 2002 and 2008 Landsat TM images, by using the hierarchical based classification method.

Roles of nonparametric classification algorithms in land use/cover classification

Nonparametric classification algorithms have some advantages over traditional algorithms in data requirement, but nonparametric algorithms often require the determination of many parameters, which is often time-consuming and challenging to optimize. The lack of clear, standardized guidelines for the determination of the parameters requires much experimentation by the analyst. For example, Artmap requires lengthy trials for identifying optimized parameters, as learning rate and vigilance. In OBC, much time is required to develop a suitable segmentation image, and intensive trials are often required to identify suitable parameters. CTA and KNN require much less time for image classification compared with Artmap and OBC because fewer parameters are used in these algorithms. This research shows that no single classification algorithm is perfect for each land use/cover type, but that each has its own merits. Therefore, it is important to develop new methods to combine the merits of different algorithms to produce a new result with high classification accuracy for each land cover type (Ceamanos et al., 2010; Chitroub, 2010; Zhu, 2010). When multisource data are used in a classification, parametric classification algorithms, such as the MLC, are typically not appropriate. Advanced nonparametric classifiers, such as decision tree, evidential reasoning, or the knowledge-based approach, appear to be the best choices.

Development of new methods for historical remote sensing image classification

Time-series Landsat images have been used for developing land-use/cover data due to their free public access (Masek et al., 2008; Vogelmann et al., 2009; Huang et al., 2010; Thomas et al., 2011). However, the limitations of remote-sensing data per se (spectral, spatial, and radiometric resolutions), atmospheric conditions, the complex vegetation composition and stand structure, and the lack of reference data that can be used for training samples during image classification make it difficult to develop high-quality time-series land-use/cover datasets (Lu & Weng, 2007). Therefore, the challenge is to develop a method to accurately map land-use/cover distribution from historical remote-sensing data without using training samples during the classification procedure. A unsupervised classification method is often used when no training samples are available. However, different analysts may produce significantly different results when merging clusters into meaningful land use/cover classes, depending on the analyst's knowledge, familiarity with the study area under investigation, and the amount of change that the area may be experiencing.

The hierarchical-based method used in this research adopts four key steps in the classification procedure: stratification of land use/cover classes to reduce the spectral confusion among different classes; the analyst's knowledge and experience from field survey, high spatial resolution images, as well as Google Earth images in addition to other ancillary data; manual editing in each step to remove the misclassified classes that could not be separated automatically from the spectral signatures; and post-processing based on bi-temporal classified images to further correct the misclassification between some land cover classes. One advantage of this method is that it does not require training samples during image classification, which is critical for land use/cover classification based on historical remote-sensing data. The disadvantage is the need for human involvement, because the analyst's experience and knowledge or familiarity with the study area might affect the classification results.

The different vegetation phenologies, atmospheric conditions, and land use/cover change history make it difficult for land use/cover classification based on historical remote sensing images. One potential solution is to develop stable and reliable variables from time-series multispectral images so that the same rules developed in the latest date images, based on training sample plots, can be transferred to historical images. Previous research has indicated that proper use of spectral mixture analysis has the potential to develop fractional images having physical meanings (Lu et al., 2003b) and has proven valuable for developing time-series impervious surface data (Lu et al., 2011c). A combination of decision tree classifier and expert knowledge may be used to classify fractional images into thematic maps.

Development of an optimal classification procedure for land use/cover classification

The success of an image classification depends on many factors, such as the availability of a sufficient number of representative sample plots, high-quality remotely sensed imagery, design of a proper classification system, geometric errors between images and sample plots, and the analyst's skills and experiences (Lu & Weng, 2007). Uncertainty and error propagation in the image-processing chain is an important factor influencing classification accuracy. Identifying the weakest linkage in the chain and then reducing the uncertainties are critical for the improvement of classification accuracy. In practice, it is often difficult to identify the best classifier for a specific study without conducting a comparative analysis of different classification algorithms. However, accuracy assessment is mainly based on test samples without further examining the spatial distribution and patterns of classification errors. It is fundamental to examine the spatial patterns of classification errors and to identify the major factors influencing classification errors in different locations, in order to take measures to reduce the errors.

The land use/cover classification is a complex procedure that may include the following steps: statement of research problem, design of a classification system, collection of ground truth data, selection of suitable remote sensing data, image preprocessing and feature selection, selection of classification algorithms, post-processing of the classified image, and accuracy assessment (Lu & Weng, 2007). Each step should be carefully designed and processed. It is also necessary to make full use of different features in remotely sensed data (e.g., spectral, spatial, and temporal) and ancillary data (e.g., DEM data in mountainous regions and population density in the urban landscape) during the classification procedure. Since different spatial resolution images are readily available, how to effectively integrate multi-scale remotely sensed data has become another research topic for improving land use/cover classification accuracy, especially for large areas.

Final considerations

Land use/cover classification in the moist tropical regions of the Brazilian Amazon is a challenge due to the complexity of the biophysical environment. The spectral signatures of remotely sensed data, for medium spatial resolution images, such as Landsat, are still the most important features in land use/cover classification. However, classification performance can be improved by the effective use of spatial features, such as textures, especially when higher spatial resolution images, such as Spot and QuickBird, are used. Data fusion of multi-resolution images, such as Landsat ETM and Spot, which have multispectral and panchromatic bands, can improve visual interpretation performance, but may not improve land use/cover classification accuracy. However, data fusion of Landsat TM and radar data (especially Palsar L-band data) improved vegetation classification. For the selection of classification algorithms, the MLC is still the common method for land use/cover classification, but some nonparametric algorithms, such as CTA, may provide better classification accuracy than the MLC, particularly when multi-source data are used. Nonparametric algorithms often require much longer time to optimize the parameters used in a specific algorithm, and the results often rely on the identified parameters and the datasets used. A sufficient number of representative sample plots are usually required for land use/cover classification; however, it is often difficult to use them for historical remote sensing image classification. Therefore, the development of new methods suitable for historical remote sensing data is especially valuable. The hierarchical-based method used in this research provides a potential solution to this issue.

Acknowledgments

To the National Institute of Child Health and Human Development and to the National Science Foundation, for financial support; and to the Japan Aerospace Exploration Agency Science Program, for providing the Alos Palsar data.

References

ALTHAUSEN, J.D. What remote sensing system should be used to collect the data? In: BOSSLER, J.D.; JENSEN, J.R.; MCMASTER, R.B.; RIZOS, C. (Ed.). **Manual of geospatial science and technology**. New York: Taylor and Francis, 2002. p.276-297.

AMOLINS, K.; ZHANG, Y.; DARE, P. Wavelet based image fusion techniques: an introduction, review and comparison. **ISPRS Journal of Photogrammetry and Remote Sensing**, v.62, p.249-263, 2007.

BATISTELLA, M.; ROBESON, S.; MORAN, E.F. Settlement design, forest fragmentation and landscape change in Rondônia, Amazônia. **Photogrammetric Engineering and Remote Sensing**, v.69, p.805-812, 2003.

BLASCHKE, T. Object based image analysis for remote sensing. **ISPRS Journal of Photogrammetry and Remote Sensing**, v.65, p.2-16, 2010.

BLASCHKE, T.; BURNETT, C.; PEKKARINEN, A. Image segmentation methods for object-based analysis and classification. In: JONG, S.M. de; MEER, F.D. van der (Ed.). **Remote sensing image analysis**: including the spatial domain. Netherlands: Kluwer Academic, 2004. p.211-236.

BRASIL. Ministério da Ciência e Tecnologia. Coordenação Geral de Orientação da Terra. **Projeto PRODES**: monitoramento da floresta amazônica brasileira por satélite. Disponível em: <http://www.obt.inpe.br/prodes/>. Acesso em: 31 out. 2012a.

BRASIL. Ministério da Ciência e Tecnologia. Coordenação Geral de Orientação da Terra. **Sistema DETER**: detecção de desmatamento em tempo real. Disponível em: <http://www.obt.inpe.br/deter/>. Acesso em: 31 out. 2012b.

CAMPS-VALLS, G.; BRUZZONE, L. **Kernel methods in remote sensing image processing**. Hoboken: John Wiley and Sons, 2009.

CAMPS-VALLS, G.; GÓMEZ-CHOVA, L.; MUÑOZ-MARÍ, J.; ROJOÁLVAREZ, J.L.; MARTÍNEZ-RAMÓN, M. Kernel-based framework for multitemporal and multisource remote sensing data classification and change detection. **IEEE Transactions on Geoscience and Remote Sensing**, v.46, p.1822-1835, 2008.

CARDILLE, J.A.; FOLEY, J.A. Agricultural land-use change in Brazilian Amazonia between 1980 and 1995: evidence from integrated satellite and census data. **Remote Sensing of Environment**, v.87, p.551-562, 2003.

CARPENTER, G.A.; GROSSBERG, S.; MARKUZON, N.; REYNOLDS, J.H.; ROSEN, D.B. Fuzzy ARTMAP: a neural network architecture for incremental supervised learning of analog multidimentional maps. **IEEE Transactions on Neural Networks**, v.3, p.698-713, 1992.

CARREIRAS, J.M.B.; PEREIRA, J.M.C.; CAMPAGNOLO, M.L.; SHIMABUKURO, Y.E. Assessing the extent of agriculture/pasture and secondary succession forest in the Brazilian Legal Amazon using SPOT VEGETATION data. **Remote Sensing of Environment**, v.101, p.283-298, 2006.

CEAMANOS, X.; WASKE, B.; BENEDIKTSSON, J.A.; CHANUSSOT, J.; FAUVEL, M.; SVEINSSON, J.R. A classifier ensemble based on fusion of support vector machines for classifying hyperspectral data. **International Journal of Image and Data Fusion**, v.1, p.293-307, 2010.

CHANDER, G.; MARKHAM, B.L.; HELDER, D.L. Summary of current radiometric calibration coefficients for Landsat MSS, TM, ETM+, and EO-1 ALI sensors. **Remote Sensing of Environment**, v.113, p.893-903, 2009.

CHIBANI, Y. Additive integration of SAR features into multispectral SPOT images by means of the à trous wavelet decomposition. **ISPRS Journal of Photogrammetry and Remote Sensing**, v.60, p.306-314, 2006.

CHITROUB, S. Classifier combination and score level fusion: concepts and practical aspects. **International Journal of Image and Data Fusion**, v.1, p.113-135, 2010.

CONGALTON, R.G. A review of assessing the accuracy of classification of remotely sensed data. **Remote Sensing of Environment**, v.37, p.35-46, 1991.

CONGALTON, R.G.; GREEN, K. **Assessing the accuracy of remotely sensed data**: principles and practices. 2nd ed. Boca Raton: CRC Press, 2008. 183p.

DONG, J.; ZHUANG, D.; HUANG, Y.; FU, J. Advances in multi-sensor data fusion: algorithms and applications. **Sensors**, v.9, p.7771-7784, 2009.

EHLERS, M.; KLONUS, S.; ASTRAND, P.J.; ROSSO, P. Multi-sensor image fusion for pansharpening in remote sensing. **International Journal of Image and Data Fusion**, v.1, p.25-45, 2010.

ELNAGGAR, A.A.; NOLLER, J.S. Application of remote-sensing data and decision-tree analysis to mapping salt-affected soils over large areas. **Remote Sensing**, v.2, p.151-165, 2010.

EORC. **ALOS**: Advanced Land Observing Satellite. Available at: <http://www.eorc.jaxa.jp/ALOS/en/about/palsar.htm>. Accessed on: 31 Oct. 2012.

FOODY, G.M. Status of land cover classification accuracy assessment. **Remote Sensing of Environment**, v.80, p.185-201, 2002.

FRANCO-LOPEZ, H.; EK, A.R.; BAUER, M.E. Estimation and mapping of forest stand density, volume, and cover type using the k-nearest neighbors method. **Remote Sensing of Environment**, v.77, p.251-274, 2001.

FRANKLIN, S.E.; WULDER, M.A. Remote sensing methods in medium spatial resolution satellite data land cover classification of large areas. **Progress in Physical Geography**, v.26, p.173-205, 2002.

FRERY, A.C.; CORREIA, A.H.; FREITAS, C. da C. Classifying multifrequency fully polarimetric imagery with multiple sources of statistical evidence and contextual information. **IEEE Transactions on Geoscience and Remote Sensing**, v.45, p.3098-3109, 2007.

GALFORD, G.L.; MUSTARD, J.F.; MELILLO, J.; GENDRIN, A.; CERRI, C.C.; CERRI, C.E.P. Wavelet analysis of MODIS time series to detect expansion and intensification of row-crop agriculture in Brazil. **Remote Sensing of Environment**, v.112, p.576-587, 2008.

HARALICK, R.M.; SHANMUGAM, K.; DINSTEIN, I. Textural features for image classification. **IEEE Transactions on Systems, Man, and Cybernetics**, v.6, p.610-620, 1973.

HARRIS, P.M.; VENTURA, S.J. The integration of geographic data with remotely-sensed imagery to improve classification in an urban area. **Photogrammetric Engineering and Remote Sensing**, v.61, p.993-998, 1995.

HEROLD, M.; LIU, X.H.; CLARKE, K.C. Spatial metrics and image texture for mapping urban land use. **Photogrammetric Engineering and Remote Sensing**, v.69, p.991-1001, 2003.

HODGSON, M.E.; JENSEN, J.R.; TULLIS, J.A.; RIORDAN, K.D.; ARCHER, C.M. Synergistic use Lidar and color aerial photography for mapping urban parcel imperviousness. **Photogrammetric Engineering and Remote Sensing**, v.69, p.973-980, 2003.

HONG, G.; ZHANG, Y. Comparison and improvement of wavelet-based image fusion. **International Journal of Remote Sensing**, v.29, p.673-691, 2008.

HUANG, C.; COWARD, S.N.; MASEK, J.G.; THOMAS, N.; ZHU, Z.; VOGELMANN, J.E. An automated approach for reconstructing recent forest disturbance history using dense Landsat time series stacks. **Remote Sensing of Environment**, v.114, p.183-198, 2010.

JENSEN, J.R. **Introductory digital image processing**: a remote sensing perspective. 3rd ed. Upper Saddle River: Prentice Hall, 2005.

KASISCHKE, E.S.; MELACK, J.M.; DOBSON, M.C. The use of imaging radars for ecological applications: a review. **Remote Sensing of Environment**, v.59, p.141-156, 1997.

KLONUS, S.; EHLERS, M. Image fusion using the Ehlers spectral characteristics preservation algorithm. **GIScience and Remote Sensing**, v.44, p.93-116, 2007.

LEFSKY, M.A.; COHEN, W.B. Selection of remotely sensed data. In: WULDER, M.A.; FRANKLIN, S.E. (Ed.). **Remote sensing of forest environments**: concepts and case studies. Boston: Kluwer Academic Publishers, 2003. p.13-46.

LI, D. Remotely sensed images and GIS data fusion for automatic change detection. **International Journal of Image and Data Fusion**, v.1, p.99-108, 2010.

LI, G.; LU, D.; MORAN, E.; HETRICK, S. Land-cover classification in a moist tropical region of Brazil with Landsat TM imagery. **International Journal of Remote Sensing**, v.32, p.8207-8230, 2011.

LI, G.; LU, D.; MORAN, E.; DUTRA, L.; BATISTELLA, M. A comparative analysis of ALOS PALSAR L-band and RADARSAT-2 C-band data for land-cover classification in a tropical moist region. **ISPRS Journal of Photogrammetry and Remote Sensing**, v.70, p.26-38, 2012.

LILLESAND, T.M.; KIEFER, R.W. **Remote sensing and image interpretation**. 4th ed. New York: Wiley, 2000. 724p.

LOBELL, D.B.; ASNER, G.P. Cropland distributions from temporal unmixing of MODIS data. **Remote Sensing of Environment**, v.93, p.412-422, 2004.

LU, D. Integration of vegetation inventory data and Landsat TM image for vegetation classification in the Western Brazilian Amazon. **Forest Ecology and Management**, v.213, p.369-383, 2005.

LU, D.; BATISTELLA, M.; MORAN, E. Integration of Landsat TM and SPOT HRG images for vegetation change detection in the Brazilian Amazon. **Photogrammetric Engineering and Remote Sensing**, v.74, p.421-430, 2008a.

LU, D.; BATISTELLA, M.; MORAN, E. Land cover classification in the Brazilian Amazon with the integration of Landsat ETM+ and RADARSAT data. **International Journal of Remote Sensing**, v.28, p.5447-5459, 2007.

LU, D.; BATISTELLA, M.; MORAN, E.; DE MIRANDA, E.E. A comparative study of Landsat TM and SPOT HRG images for vegetation classification in the Brazilian Amazon. **Photogrammetric Engineering and Remote Sensing**, v.74, p.311-321, 2008b.

LU, D.; BATISTELLA, M.; MORAN, E.; HETRICK, S.; ALVES, D.; BRONDIZIO, E. Fractional forest cover mapping in the Brazilian Amazon with a combination of MODIS and TM images. **International Journal of Remote Sensing**, v.32, p.7131-7149, 2011a.

LU, D.; BATISTELLA, M.; MORAN, E.; MAUSEL, P. Application of spectral mixture analysis to Amazonian land-use and land-cover classification. **International Journal of Remote Sensing**, v.25, p.5345-5358, 2004a.

LU, D.; HETRICK, S.; MORAN, E. Land cover classification in a complex urban-rural landscape with QuickBird imagery. **Photogrammetric Engineering and Remote Sensing**, v.76, p.1159-1168, 2010.

LU, D.; HETRICK, S.; MORAN, E.; LI, G. Application of time series Landsat images to examining land use/cover dynamic change. **Photogrammetric Engineering and Remote Sensing**, v.78, p.747-755, 2012.

LU, D.; LI, G.; MORAN, E.; DUTRA, L.; BATISTELLA, M. A comparison of multisensor integration methods for land-cover classification in the Brazilian Amazon. **GIScience and Remote Sensing**, v.48, p.345-370, 2011b.

LU, D.; MAUSEL, P.; BATISTELLA, M.; MORAN, E. Comparison of land-cover classification methods in the Brazilian Amazon basin. **Photogrammetric Engineering and Remote Sensing**, v.70, p.723-731, 2004b.

LU, D.; MAUSEL, P.; BRONDÍZIO, E.; MORAN, E. Assessment of atmospheric correction methods for Landsat TM data applicable to Amazon basin LBA research. **International Journal of Remote Sensing**, v.23, p.2651-2671, 2002.

LU, D.; MAUSEL, P.; BRONDÍZIO, E.; MORAN, E. Classification of successional forest stages in the Brazilian Amazon basin. **Forest Ecology and Management**, v.181, p.301-312, 2003a.

LU, D.; MORAN, E.; BATISTELLA, M. Linear mixture model applied to Amazonian vegetation classification. **Remote Sensing of Environment**, v.87, p.456-469, 2003b.

LU, D.; MORAN, E.; HETRICK, S. Detection of impervious surface change with multitemporal Landsat images in an urban-rural frontier. **ISPRS Journal of Photogrammetry and Remote Sensing**, v.66, p.298-306, 2011c.

LU, D.; WENG, Q. A survey of image classification methods and techniques for improving classification performance. **International Journal of Remote Sensing**, v.28, p.823-870, 2007.

MANNAN, B.; ROY, J.; RAY, A.K. Fuzzy ARTMAP supervised classification of multi-spectral remotely-sensed images. **International Journal of Remote Sensing**, v.19, p.767-774, 1998.

MARCEAU, D.J.; HOWARTH, P.J.; DUBOIS, J.M.; GRATTON, D.J. Evaluation of the grey-level co-occurrence matrix method for land-cover classification using SPOT imagery. **IEEE Transactions on Geoscience and Remote Sensing**, v.28, p.513-519, 1990.

MASEK, J.G.; HUANG, C.; WOLFE, R.; COHEN, W.; HALL, F.; KUTLER, J.; NELSON, P. North American forest disturbance mapped from a decadal Landsat record. **Remote Sensing of Environment**, v.112, p.2914-2926, 2008.

MASELLI, F.; CHIRICI, G.; BOTTAI, L.; CORONA, P.; MARCHETTI, M. Estimation of Mediterranean forest attributes by the application of K-NN procedures to multitemporal Landsat ETM+ images. **International Journal of Remote Sensing**, v.26, p.3781-3796, 2005.

MCROBERTS, R.R.; TOMPPO, E.O. Remote sensing support for national forest inventories. **Remote Sensing of Environment**, v.110, p.412-419, 2007.

MICHELSON, D.B.; LILJEBERG, B.M.; PILESJO, P. Comparison of algorithms for classifying Swedish landcover using Landsat TM and ERS-1 SAR data. **Remote Sensing of Environment**, v.71, p.1-15, 2000.

MILLER, J.; FRANKLIN, J. Modeling the distribution of four vegetation alliances using generalized linear models and classification trees with spatial dependence. **Ecological Modelling**, v.157, p.227-247, 2002.

MORAN, E.F.; BRONDÍZIO, E.S. Land-use change after deforestation in Amazônia. In: LIVERMAN, D.; MORAN, E.F.; RINDFUSS, R.R.; STERN, P.C. (Ed.). **People and pixels**: linking remote sensing and social science. Washington: National Academy Press, 1998. p.94-120.

MORAN, E.F.; BRONDÍZIO, E.S.; MAUSEL, P.; WU, Y. Integrating Amazonian vegetation, land-use, and satellite data. **Bioscience**, v.44, p.329-338, 1994.

MOUNTRAKIS, G.; IM, J.; OGOLE, C. Support vector machines in remote sensing: a review. **ISPRS Journal of Photogrammetry and Remote Sensing**, v.66, p.247-259, 2011.

PAL, M.; MATHER, P.M. An assessment of the effectiveness of decision tree methods for land cover classification. **Remote Sensing of Environment**, v.86, p.554-565, 2003.

PAL, M.; MATHER, P.M. Assessment of the effectiveness of support vector machines for hyperspectral data. **Future Generation Computer System**, v.20, p.1215-1225, 2004.

PERUMAL, K.; BHASKARAN, R. SVM-based effective land use classification system for multispectral remote sensing images. **International Journal of Computer Science and Information Security**, v.6, p.97-105, 2009.

POHL, C.; VAN GENDEREN, J.L. Multisensor image fusion in remote sensing: concepts, methods, and applications. **International Journal of Remote Sensing**, v.19, p.823-854, 1998.

ROGAN, J.; FRANKLIN, J.; STOW, D.; MILLER, J.; WOODCOCK, C.; ROBERTS, D. Mapping land-cover modifications over large areas: a comparison of machine learning algorithms. **Remote Sensing of Environment**, v.112, p.2272-2283, 2008.

SANO, E.E.; ROSA, R.; BRITO, J.L.S.; FERREIRA, L.G. Land cover mapping of the tropical savanna region in Brazil. **Environmental Monitoring and Assessment**, v.166, p.113-124, 2010.

STEFANOV, W.L.; RAMSEY, M.S.; CHRISTENSEN, P.R. Monitoring urban land cover change: an expert system approach to land cover classification of semiarid to arid urban centers. **Remote Sensing of Environment**, v.77, p.173-185, 2001.

THOMAS, N.E.; HUANG, C.; GOWARD, S.N.; POWELL, S.; RISHMAWI, K.; SCHLEEWEIS, K.; HINDS, A. Validation of North American forest disturbance dynamics derived from Landsat time series stacks. **Remote Sensing of Environment**, v.115, p.19-32, 2011.

TOMPPO, E.; HALME, M. Using coarse scale forest variables as ancillary information and weighting of variables in k-NN estimation: a genetic algorithm approach. **Remote Sensing of Environment**, v.92, p.1-20, 2004.

TSO, B.; MATHER, P.M. **Classification methods for remotely sensed data**. London: Taylor and Francis, 2001. 332p.

TUIA, D.; MUÑOZ-MARÍ, J.; KANEVSKI, M.; CAMPS-VALLS, G. Structured output SVM for remote sensing image classification. **Journal of Signal Processing Systems**, v.65, p.457-468, 2011.

VOGELMANN, J.E.; TOLK, B.; ZHU, Z. Monitoring forest changes in the southwestern United States using multitemporal Landsat data. **Remote Sensing of Environment**, v.113, p.1739-1748, 2009.

WARDLOW, B.D.; EGBERT, S.L. Large-area crop mapping using time-series MODIS 250 m NDVI data: an assessment for the U.S. Central Great Plains. **Remote Sensing of Environment**, v.112, p.1096-1116, 2008.

YU, Q.; GONG, P.; CLINTON, N.; BIGING, G.; KELLY, M.; SCHIROKAUER, D. Object-based detailed vegetation classification with airborne high spatial resolution remote sensing imagery. **Photogrammetric Engineering and Remote Sensing**, v.72, p.799-811, 2006.

ZAMBON, M.; LAWRENCE, R.; BUNN, A.; POWELL, S. Effect of alternative splitting rules on image processing using classification tree analysis. **Photogrammetric Engineering and Remote Sensing**, v.72, p.25-30, 2006.

ZHANG, J. Multisource remote sensing data fusion: status and trends. **International Journal of Image and Data Fusion**, v.1, p.5-24, 2010.

ZHU, D. A hybrid approach for efficient ensembles. **Decision Support Systems**, v.48, p.480487, 2010.

Received on July 30, 2012 and accepted on August 31, 2012